Recent multivariate changes in the North Atlantic climate system, with a focus on 2005-2016

Robson, J. ORCID: https://orcid.org/0000-0002-3467-018X, Sutton, R. T. ORCID: https://orcid.org/0000-0001-8345-8583, Archibald, A., Cooper, F., Christensen, M., Gray, L. J., Holliday, N. P., Macintosh, C., McMillan, M., Moat, B., Russo, M., Tilling, R., Carslaw, K., Desbruyères, D., Embury, O. ORCID: https://orcid.org/0000-0002-1661-7828, Feltham, D. L. ORCID: https://orcid.org/0000-0003-2289-014X, Grosvenor, D. P., Josey, S., King, B., Lewis, A., McCarthy, G. D., Merchant, C. ORCID: https://orcid.org/0000-0003-4687-9850, New, A. L., O'Reilly, C. H., Osprey, S. M., Read, K., Scaife, A., Shepherd, A., Sinha, B., Smeed, D., Smith, D., Ridout, A., Woollings, T. and Yang, M. (2018) Recent multivariate changes in the North Atlantic climate system, with a focus on 2005-2016. International Journal of Climatology, 38 (12). pp. 5050-5076. ISSN 0899-8418 doi: 10.1002/joc.5815 Available at https://centaur.reading.ac.uk/78967/

Received: 22 December 2017 | Revised: 13 June 2018 | Accepted: 17 July 2018

DOI: 10.1002/joc.5815

International Journal of Climatology RMetS

REVIEW

Recent multivariate changes in the North Atlantic climate system, with a focus on 2005–2016

Jon Robson[1] | Rowan T. Sutton[1] | Alex Archibald[2] | Fenwick Cooper[3] | Matthew Christensen[4,3] | Lesley J. Gray[3] | N. Penny Holliday[5] | Claire Macintosh[6] | Malcolm McMillan[7] | Ben Moat[5] | Maria Russo[2] | Rachel Tilling[7] | Ken Carslaw[8] | Damien Desbruyères[5,9] | Owen Embury[6] | Daniel L. Feltham[10] | Daniel P. Grosvenor[8] | Simon Josey[5] | Brian King[5] | Alastair Lewis[11] | Gerard D. McCarthy[5,12] | Chris Merchant[6] | Adrian L. New[5] | Christopher H. O'Reilly[3] | Scott M. Osprey[3] | Katie Read[11] | Adam Scaife[13,14] | Andrew Shepherd[7] | Bablu Sinha[5] | David Smeed[5] | Doug Smith[13] | Andrew Ridout[15] | Tim Woollings[3] | Mingxi Yang[16]

[1]National Centre for Atmospheric Science, Department of Meteorology, University of Reading, Reading, UK

[2]National Centre for Atmospheric Science, Department of Chemistry, University of Cambridge, Cambridge, UK

[3]Atmosphere, Ocean and Planetary Physics, University of Oxford, Oxford, UK

[4]STFC Rutherford Appleton Laboratory, Oxford, UK

[5]National Oceanography Centre, Southampton, UK

[6]National Centre for Earth Observation, Department of Meteorology, University of Reading, Reading, UK

[7]Centre for Polar Observations and Modelling, University of Leeds, Leeds, UK

[8]National Centre for Atmospheric Science, School of Earth and Environment, University of Leeds, Leeds, UK

[9]IFREMER, Laboratoire d'Océanographie Physique et Spatiale, Plouzané, France

[10]Centre for Polar Observations and Modelling, Department of Meteorology, University of Reading, Reading, UK

[11]National Centre for Atmospheric Science, University of York, York, UK

[12]Irish Climate Analysis and Research UnitS (ICARUS), Department of Geography, National University of Ireland Maynooth, Maynooth, Ireland

[13]Met Office Hadley Centre, Exeter, UK

[14]College of Engineering, Maths and Physical Science, University of Exeter, Exeter, UK

[15]Centre for Polar Observations and Modelling, University College London, London, UK

[16]Plymouth Marine Laboratory, Plymouth, UK

Correspondence
Jon Robson, National Centre for Atmospheric Science, Department of Meteorology, University of Reading, Reading, UK.
Email: j.i.robson@reading.ac.uk

Funding information
Natural Environment Research Council, Grant/Award Number: North Atlantic Climate System: Integrated Study (ACSIS)

Major changes are occurring across the North Atlantic climate system, including in the atmosphere, ocean and cryosphere, and many observed changes are unprecedented in instrumental records. As the changes in the North Atlantic directly affect the climate and air quality of the surrounding continents, it is important to fully understand how and why the changes are taking place, not least to predict how the region will change in the future. To this end, this article characterizes the recent observed changes in the North Atlantic region, especially in the period 2005–2016, across many different aspects of the system including: atmospheric circulation; atmospheric composition; clouds and aerosols; ocean circulation and properties; and the cryosphere. Recent changes include: an increase in the speed of the North Atlantic jet stream in winter; a southward shift in the North Atlantic jet stream in summer, associated with a weakening summer North Atlantic Oscillation; increases

in ozone and methane; increases in net absorbed radiation in the mid-latitude western Atlantic, linked to an increase in the abundance of high level clouds and a reduction in low level clouds; cooling of sea surface temperatures in the North Atlantic subpolar gyre, concomitant with increases in the western subtropical gyre, and a decline in the Atlantic Ocean's overturning circulation; a decline in Atlantic sector Arctic sea ice and rapid melting of the Greenland Ice Sheet. There are many interactions between these changes, but these interactions are poorly understood. This article concludes by highlighting some of the key outstanding questions.

KEYWORDS

atmosphere, atmospheric composition, cryosphere, observations, ocean, north atlantic

1 | INTRODUCTION

The North Atlantic region has warmed over the past 100 or so years (Stocker *et al.,* 2013; Cheng *et al.,* 2017). However, the North Atlantic has also evolved somewhat differently to the rest of the world's oceans on multidecadal time scales, with periods of faster warming and cooling. This variability, which has become known as Atlantic multidecadal variability (AMV, Sutton *et al.,* 2017), has been linked to a wide range of impacts including rainfall anomalies over Africa, North America and Europe (Sutton and Hodson, 2005; Knight *et al.,* 2006; Sutton and Dong, 2012); the frequency of Hurricanes (Zhang and Delworth, 2006; Smith *et al.,* 2010); the rate of Greenland ice-sheet melt (Holland *et al.,* 2008; Hanna *et al.,* 2013a); sea-level anomalies (McCarthy et al., 2015); fisheries (Hátún *et al.,* 2009) and the strength of the mid-latitude atmospheric jet (Woollings *et al.,* 2015). Therefore, uncertainty in how North Atlantic surface temperatures might change is a major uncertainty in climate projections, especially for the European sector (Woollings *et al.,* 2012).

Although multidecadal variability has been observed in the North Atlantic, the mechanisms and processes that control this variability are poorly understood. A leading hypothesis is that changes in the strength of the ocean circulation, and particularly the Atlantic meridional overturning circulation (AMOC), is an important contributor to the variability in the ocean heat content and sea surface temperature (SST) (Knight, 2005; Ba *et al.,* 2014; Menary *et al.,* 2015). However, although indirect observations suggest ocean circulation has led AMV-related changes in the North Atlantic (McCarthy et al., 2015; Robson *et al.,* 2016; Thornalley *et al.,* 2018), a paucity of observations has prevented a direct link being made between ocean circulation changes and AMV in the real world. There is also a considerable diversity in the mechanisms of variability found in climate models and the important feedbacks that control the time scales of variability (Ba *et al.,* 2014; Menary *et al.,* 2015).

Variability in the atmospheric circulation is also an important driver of climate variability across the North Atlantic climate system. The leading mode of atmospheric variability, the North Atlantic Oscillation (NAO), drives inter-annual to multidecadal time-scale variability in variables that span the entire Atlantic climate system, including SST, ocean circulation, troposhperic ozone, surface run off from Greenland and extreme temperatures and rainfall over Europe (Hurrell *et al.,* 2003; Scaife *et al.,* 2008; Pausata *et al.,* 2012; Robson *et al.,* 2012; Hanna *et al.,* 2014). Indeed, the NAO is often considered a major driver of AMOC, and hence AMV (Eden and Willebrand, 2001; Robson *et al.,* 2012; Delworth and Zeng, 2016; Sutton *et al.,* 2017)—although it has also been hypothesised that the NAO may drive AMV with no need for ocean circulation changes (Clement *et al.,* 2015). On decadal time scales, the NAO may also be influenced by AMV or other changes in North Atlantic conditions such as regional SST anomalies or sea ice changes (Gastineau *et al.,* 2013; Gastineau and Frankignoul, 2014; Peings and Magnusdottir, 2014; O'Reilly *et al.,* 2017; Wang *et al.,* 2017). However, unravelling the interactions between ocean, atmosphere and cryosphere is very challenging, especially in the short observational record.

A further question to consider is the role of external factors in driving changes in the North Atlantic. For example, recent studies have suggested that AMV is a result of competition between rising greenhouse gas emissions and regional changes in sulphate aerosols (Booth *et al.,* 2012). Changes in solar irradiance and volcanic aerosols are also thought to be important influences on the atmospheric circulation and the NAO, and hence could impact widely across the North Atlantic climate system (Gray *et al.,* 2013; Menary *et al.,* 2013; Ortega *et al.,* 2015). The long-term warming trend is also changing the climate of the North Atlantic region, especially in the high latitudes, including melting Arctic sea ice and the Greenland Ice sheet (Stocker *et al.,* 2013) which could influence the oceanic (Swingedouw *et al.,* 2013) and atmospheric (Screen *et al.,* 2018)

circulation. Finally, the presence of global teleconnections, in the atmosphere in particular, means that variability and changes outside the North Atlantic can also have a substantial influence (Biastoch *et al.,* 2008; Bell *et al.,* 2009).

The composition of the atmosphere in the North Atlantic region has also been changing, and can interact with changes in physical aspects of the climate. Ozone (O_3) and methane (CH_4) are powerful greenhouse gases and can affect climate by changing the Earth's radiative balance (Stocker *et al.,* 2013). Tropospheric ozone can also affect human health and agricultural yields (Kampa and Castanas, 2008), and was recently suggested to cause 1.2 million premature deaths per year (Malley *et al.,* 2017). Observed ozone changes are driven by a complex interplay of emission changes in nitrogen oxides and organic and inorganic radicals, changes in downward transport from the stratosphere, and changes in regional atmospheric circulation affecting transport time scales (see. e.g., Monks *et al*. (2015) for more details). However, while recent trends in carbon monoxide and methane are generally driven by emission changes (Worden *et al.,* 2013; Nisbet *et al.,* 2016), the recent observed trends in ozone over the North Atlantic are not fully characterized or understood (Parrish *et al.,* 2014) and require a deeper understanding of relationships to atmospheric circulation changes.

It follows from the above discussion that there are many important unanswered questions regarding the nature of decadal timescale change in the North Atlantic region, and how changes in different components of the North Atlantic climate system are interlinked. This lack of understanding is a fundamental limit to our ability to understand the current changes, and to our ability to make quantitative predictions of how the North Atlantic climate system will change in the future. However, the large number of important variables and processes involved in the changes, and the complex array of interactions between different components of the North Atlantic climate system, makes understanding the ongoing changes across all components of the North Atlantic climate system extremely challenging. Therefore, there is a need to take a more holistic, and multidisciplinary, view of decadal time-scale variability in the North Atlantic. Therefore, with this end in mind, this article aims to broadly characterize and document the observed changes across multiple components of the North Atlantic climate system in one place, and to review of the relevant recent literature. Although the atmosphere has been well observed for many decades, other important variables have not. Therefore, we focus on the observed changes over the recent time period (since 2000) by exploiting the many new observations and improved reanalysis products that have recently become available as a consequence of programmes such as ARGO and RAPID, and satellite products. The period 2006–2015/2016 is a particular focus due to the vastly improved data coverage over all components of the North Atlantic.

This article is structured as follows. Recent changes in atmospheric circulation are described in Section 2, before recent changes in atmospheric composition are discussed in Section 3. Recent changes in aerosols, clouds and radiative effects are described in Section 4, before changes in ocean properties and the cryosphere are discussed in Sections 5 and 6. Finally, a summary and conclusions are presented in Section 7.

2 | RECENT CHANGES IN ATMOSPHERIC CIRCULATION AND PROPERTIES

In this section, we consider the recent variability and trends in atmospheric circulation over the North Atlantic region. We use data from the European Centre for Medium-Range Weather Forecasts ERA-interim reanalysis (Dee *et al.,* 2011) and, where stated, from the Atmospheric and InfraRed Sounder (AIRS) instrument onboard NASA's Aqua satellite (Tian *et al.,* 2017).

"The North Atlantic Oscillation (NAO) is one of the most prominent and recurrent patterns of atmospheric circulation variability" (Hurrell *et al.,* 2003). It is usually defined as the first empirical orthogonal function (EOF) of surface pressure in the region 30°W–40°E and 20°–70°N and its time evolution can be illustrated by plotting the corresponding principal component time series. An alternative that does not require knowledge of surface pressure over this extended region uses the normalized pressure difference between station-based observations, usually between Azores-Iceland (Hurrell, 1995; Cropper *et al.,* 2015) or between Reykjavík–Gibraltar, (Jones *et al.,* 1997). We employ the Reykjavík–Gibraltar ($NAO_{R\text{-}G}$) index here. The standard EOF-based NAO and the $NAO_{R\text{-}G}$ indicators are very similar in the winter season [December–January–February (DJF)], with a correlation coefficient of 0.89 over the period 1979–2016.

The recent $NAO_{R\text{-}G}$ index averaged over the winter months (DJF) is plotted in Figure 1a. The smoothed 11-year running mean of $NAO_{R\text{-}G}$ increases from the mid-1980s, peaks around the early 1990s, and is followed by a downward trend (Woollings *et al.,* 2015). The winter of DJF 2009/2010 exhibits a particularly strong negative NAO, although positive values in the more recent years may indicate a positive trend. To focus more on how the atmospheric circulation has varied over the North Atlantic Ocean, we also derive an EOF-based index of the NAO (NAO_{Atl}) using the first EOF of surface pressure over the restricted region centred over the Atlantic, that is, 60°–0°W and 30°–70°N (Figure 1b; see also Figure S1a, Supporting Information). In comparison with $NAO_{R\text{-}G}$, the 11-year running mean of NAO_{Atl} in DJF is noticeably flatter with respect to its variance, although the correlation of the DJF NAO_{Atl} with $NAO_{R\text{-}G}$ is still 0.82. The 11-year running mean of NAO_{Atl} for the summer months (June–July–August; JJA; Figure 1c, with corresponding EOF in Figure S1c) has been on a

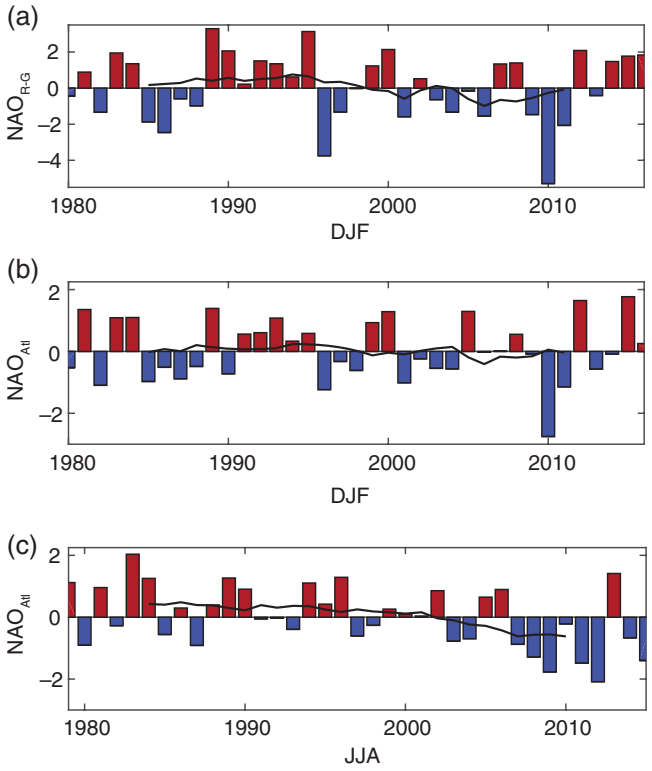

FIGURE 1 (a) NAO index estimated from the normalized difference of surface pressures at Reykjavik and Gibraltar. Each of the surface pressure time series is normalized by their respective standard deviation (SD), so the index is dimensionless. (b) DJF Atlantic NAO index estimated as the surface pressure principal component time series over the region 60°–0°W, 30°–70°N. The principal component time series is normalized by its *SD*, so the index is dimensionless. (c) JJA Atlantic NAO index otherwise as (b). All plots: The bars indicate the seasonal mean values and the thick black line indicates an 11-year running mean [Colour figure can be viewed at wileyonlinelibrary.com]

continuous downward trend since 1990 and was previously reported as statistically significant (Hanna *et al.,* 2015). (We note from examination of the structure of the first EOF of the JJA surface pressure that the station-based NAO_{R-G} is not an appropriate indicator of the summer-time circulation [compare A2a and A2b.] and it is therefore not shown).

While the NAO is a useful single indicator of atmospheric circulation over the Atlantic and its potential impact on European weather, it is nevertheless a derived quantity combining several factors. Two additional indicators that directly characterize the North Atlantic Jetstream have been proposed: the jet latitude and jet speed (Woollings *et al.,* 2014). Figure 2a,b shows the DJF and JJA time series of zonal velocity at 850 hPa in the region 60°–0°W and 15°–75°N, to illustrate the spatial evolution of the mid-latitude Jetstream. The jet latitude index (JLI) is defined as the latitude of the maximum zonal wind speed at 850 hPa calculated using seasonal mean zonal winds over the region 60°–0°W, 15°–75°N (Figure 2c,d). The JLI is clearly related to NAO_{Atl} (compare Figures 1b,c and 2c,d); positive NAO_{Atl} implies that the jet maximum is somewhat offset to the north. Figure 2c shows that recent trends in the 11-year running mean of the winter JLI are small in comparison with the interannual variability (Woollings *et al.,* 2014). However, the 1979–2015 southward trend in summer JLI (Figure 2d) is statistically significant at the $p < .05\%$ level, consistent with the negative trend in the NAO_{Atl} in JJA (Figure 1c). Note the different scales in Figure 2c,d indicating that variability in winter JLI is larger than in summer.

The jet speed index (Figure 2e,f) is defined as the maximum zonal velocity in the region 60°–0°W at the latitude identified by the JLI. It is also more variable in winter than in summer. The 11-year running mean of the winter jet speed peaks in 1990, is a minimum around 2005, and then returns to higher speeds more recently. As the summertime jet has moved southwards in recent years it has also weakened (Figure 2f). Figure 2f also hints that variability in the JJA mean jet speed has reduced.

Comparing the NAO and jet indices, we can see that the negative summer NAO trend over 2005–2016 (Figure 1c) largely reflecting an equatorward jet shift (Figure 2d), with some contribution of a weaker jet (Figure 2f). In the winter, the trend over 2005–2016 was to a slightly stronger jet (Figure 2e). However, the interannual variability in jet latitude (Figure 2c) also made an important contribution to the interannual evolution of the NAO (Figure 1a). An increase in the year-to-year variability of the December NAO (Hanna *et al.,* 2015) and corresponding jet latitude (Overland *et al.,* 2015) has also been reported previously. The equatorward migration of the summertime jet may be linked to AMV (Sutton and Dong, 2012), which transitioned from negative to positive in the mid-1990s (Sutton *et al.,* 2017). Nevertheless, these changes in the zonal wind speed and latitude have implications for atmospheric heat and water vapour (Deser *et al.,* 2010) and aerosol (Lewis and Schwartz, 2004) exchange with the Atlantic Ocean, as has been pointed out for the Southern Ocean (Korhonen *et al.,* 2010).

Figure 3 shows trends in the overall seasonal surface pressure fields (rather than only the NAO index). In DJF for both the 1990–2005 and 2006–2016 periods, the pressure trends project strongly onto the second EOF pattern. The dot products of these trends with the second EOF patterns (not shown), both normalized to unit vectors, are 81 and 76%, respectively, while their projection onto the first EOF pattern is weaker (19 and 51%, respectively). In JJA on the other hand, the situation is reversed with stronger projection of trends onto the first EOF (55 and 56%, respectively) than onto the second EOF (17 and 12%, respectively).

In Figure 3, the hatched regions indicate where there is less than a 5% chance (i.e., $p \leq .05$) that the observed trend is consistent with random variability. We conclude that trends in the seasonal mean surface pressure over the periods considered are small relative to its variance, and the trends will be sensitive to the time periods used. However, over the period 1990–2005, there was a statistically significant increase in pressure over Greenland (also noted by Hanna

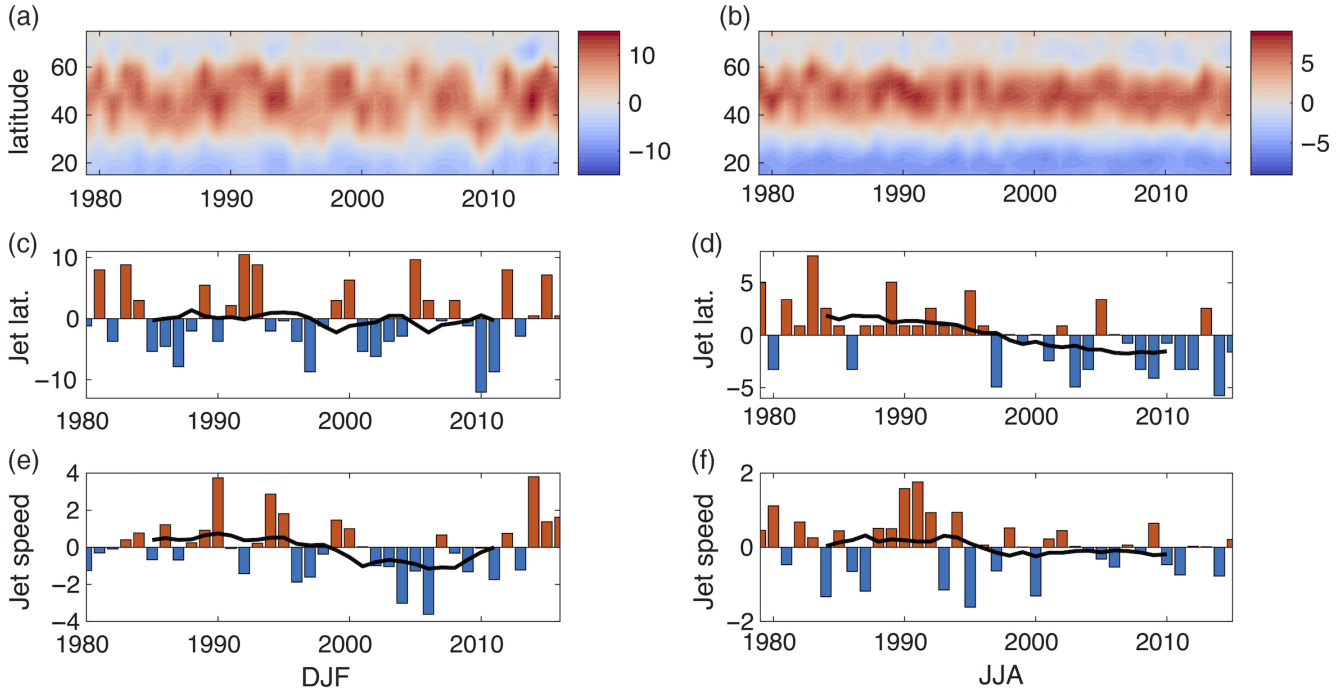

FIGURE 2 Top row: (a) and (b), seasonal and longitudinal average of the zonal velocity as a function of latitude at 850 hPa in the region 60°–0°W, (m/s). Note the change in colour scale. Middle row: (c) and (d), latitude anomaly (degrees) of the maximum of the seasonal mean zonal velocity at 850 hPa in the region 60°–0°W, 15–75°N. Bottom row: (e) and (f), anomaly of the maximum of the seasonal mean zonal velocity (m/s) at 850 hPa in the region 60°–0°W, 15°–75°N. Left: Index averaged over DJF. Right: Index averaged over JJA. All plots: The bars indicate the monthly mean values and the thick black line indicates an 11-year running mean [Colour figure can be viewed at wileyonlinelibrary.com]

et al., 2016). This increase suggests that the 11-year decreasing trend in NAO over this period (Figure 1a,b) is potentially associated with a weakening of the Icelandic Low (i.e., the northern node of the NAO). Despite a stronger (positive) trend over 2006–2016 when compared to 1989–2005, the 2006–2016 trend is not significantly different from that expected from random numbers (note also the slightly shorter time period). The summertime pressure trends are smaller than the wintertime trends, but note that this could be due to the smaller variability in summertime.

As an illustration of the vertical distribution of recent circulation changes, Figure 4 shows the zonally averaged DJF zonal wind at 60°N. Year-to-year changes in the strength of the extratropical westerly jet stream tend to be equivalent barotropic and hence vertically aligned throughout the depth of the troposphere and stratosphere. There is also sometimes additional evidence for a downward propagation of zonal wind changes and they show some striking inter-decadal variability. Recent decades have shown substantial variability in the strength of these extratropical winter westerlies. A build-up of strong westerlies occurred from the early 1960s (see, e.g., Figure 3 in Scaife *et al.* (2005), and also Hanna *et al.* (2008a) in relation to "storminess"), and is apparent throughout the depth of the atmosphere, eventually peaking in the early 1990s, as evident in Figure 4. These early 1990s winters also coincided with a string of positive episodes of the surface NAO and were accompanied by intense storms, very wet winters and a drastic reduction in the number of frost days in northern Europe (Scaife *et al.,* 2008; Roberts *et al.,* 2014). While the build-up of the westerlies in the early 1990s seen in Figure 4 is related to multidecadal variability rather than a systematic trend, the reasons are still unclear. It is not even known if this is due to forced or internal variability. The proposed explanations involve internal chaotic variability (Semenov *et al.,* 2008), ocean–atmosphere interaction (Hoerling *et al.,* 2004; Omrani *et al.,* 2016) and forced responses to volcanism (Marshall and Scaife, 2009; Driscoll *et al.,* 2012) or solar variability (Gray *et al.,* 2010; Ineson *et al.,* 2011).

Following the peak winter westerlies in the early 1990s seen in Figure 4, a subsequent decline is evident, with a deep minimum in 2010 that corresponds to the strongly negative NAO in Figure 1a,b. Although the maximum easterly anomalies are in the troposphere, there is evidence of downward extension from the stratosphere. The 2010 anomaly is also visible as an equatorward shift in the position of the Atlantic westerlies (Figure 2a). The winter of 2009/2010 exhibited the lowest NAO on record (Cattiaux *et al.,* 2010; Seager *et al.,* 2010; Fereday *et al.,* 2012) and followed in 2010 by the coldest December for a century (Maidens *et al.,* 2013; Blaker *et al.,* 2015). Potential causes of the 2009/2010 weak westerlies includes the extratropical response to El Nino (Fereday *et al.,* 2012), the deep minimum in the 11-year solar cycle (Gray *et al.,* 2013, 2016), the easterly phase of the quasi-biennial oscillation (QBO) (Pascoe *et al.,* 2006; Fereday *et al.,* 2012), and Arctic sea-ice losses (Strong and Magnusdottir, 2011; Wang *et al.,* 2017).

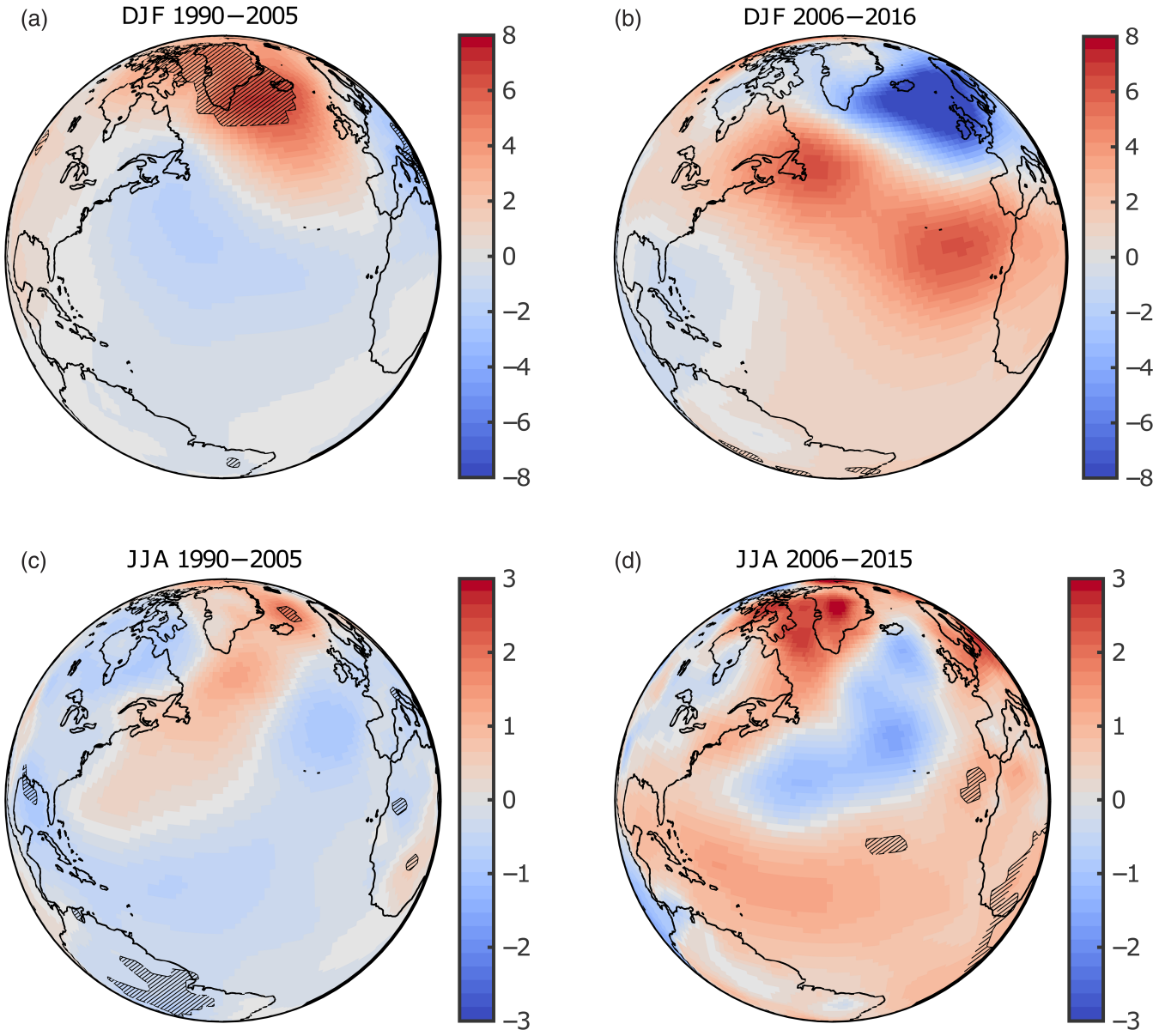

FIGURE 3 Trends in the seasonal mean surface pressure in hPa per decade. Hatched regions are where the trend exceeds the 95% confidence interval for Gaussian distributed random numbers, with one number per season [Colour figure can be viewed at wileyonlinelibrary.com]

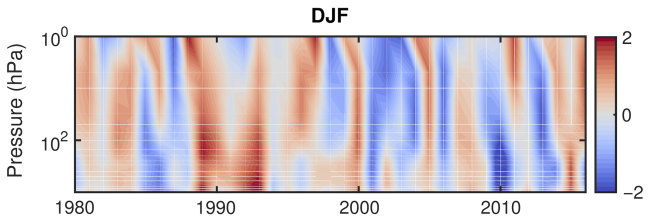

FIGURE 4 Seasonal average of the DJF zonal mean zonal wind anomaly at 60N (m/s). The time series on each pressure level has been normalized to have a *SD* of one in order to highlight the barotropic nature of the flow [Colour figure can be viewed at wileyonlinelibrary.com]

After 2010, the westerlies strengthened again. The recent three winters from 2013/2014 to 2015/2016 were all strong westerly winters with positive surface NAO and numerous winter wind storms and abundant rainfall (Huntingford *et al.,* 2014; Wild *et al.,* 2015; Watson *et al.,* 2016; Scaife *et al.,* 2017). Recent changes in the Atlantic Ocean surface conditions and tropical rainfall help to explain this recent upturn, which also closely follows the recent solar maximum (Scaife *et al.,* 2017).

North Atlantic SSTs are strongly influenced by atmospheric seasonal variability (see Section 5 of this article and, e.g., Deser *et al.,* 2010). However, surface heat fluxes are governed by a complex function of the wind speed, humidity and temperature differences (e.g., Hewitt *et al.,* 2011, their Figure 1). The 2006–2016 trend in ERA-interim 2 m temperature is plotted in Figure 5a,b (DJF, JJA, respectively). The DJF cooling in the North Atlantic region is visible above the background variability, consistent with the 1996–2005 SST trends in Figure 14. The summertime trend (JJA) over this time period is smaller, but shows the same overall pattern of a cooling in the north Atlantic, including over Greenland, and a warming further towards the tropics.

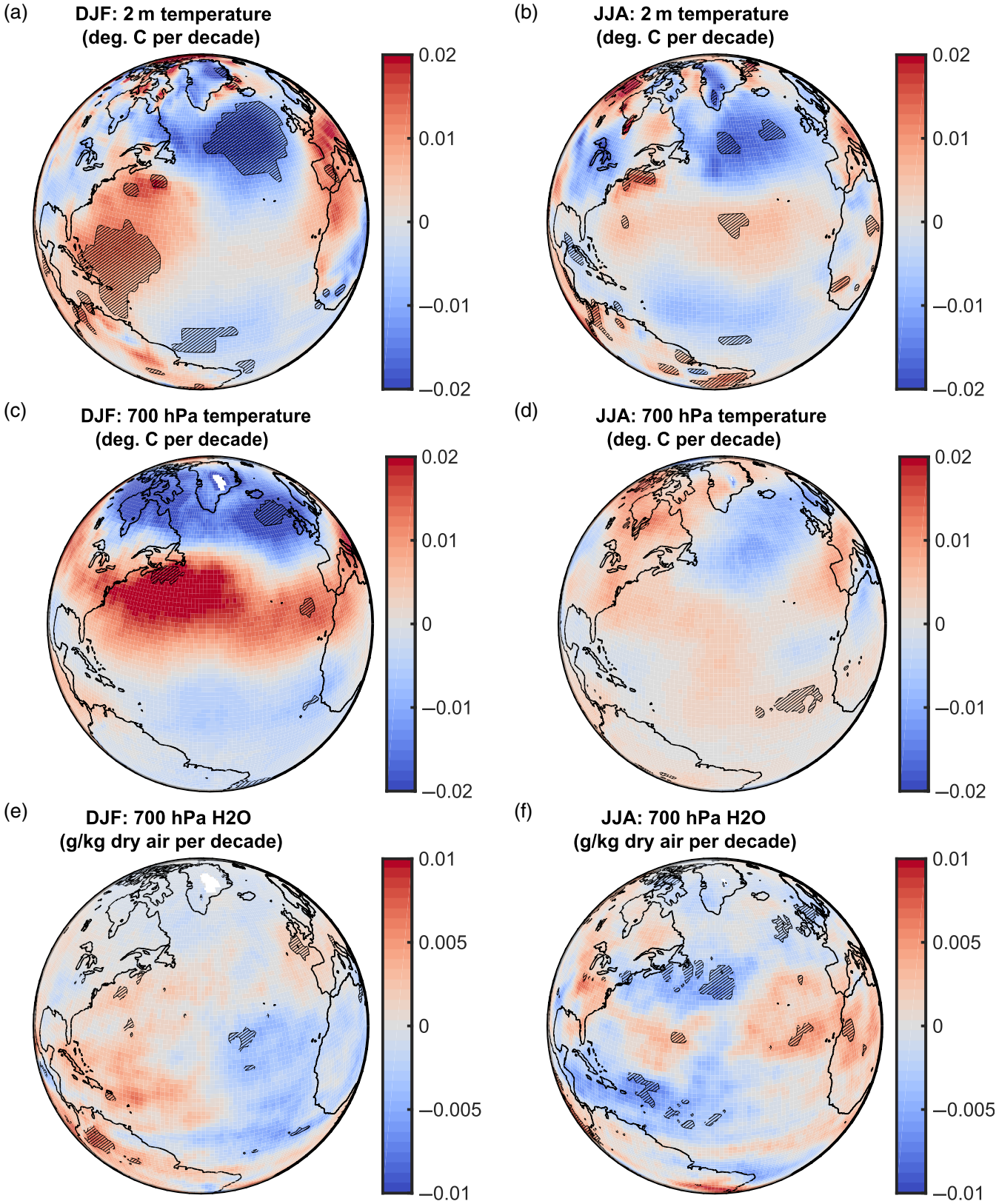

FIGURE 5 Decadal trends over the period 2006–2016. Top row: (a) and (b), 2 m air temperature trend using ERA-interim data. Middle row: (c) and (d), 700 hPa temperature, as measured by AIRS, see http://airs.jpl.nasa.gov. Bottom row: (e) and (f), 700 hPa water mass mixing ratio, as measured by AIRS [Colour figure can be viewed at wileyonlinelibrary.com]

To examine trends at higher levels, the 2006–2016 trends in the seasonal mean 700 hPa air temperature are plotted in Figure 5c,d (now as measured by AIRS, to be consistent with the water mass mixing ratio plots in Figure 5e,f). Although barely distinguishable from the background variability, both the wintertime and summer time 700 hPa trends bear some resemblance to their 2 m equivalents. In DJF, the north Atlantic has cooled at 700 hPa by around 0.15 °C per

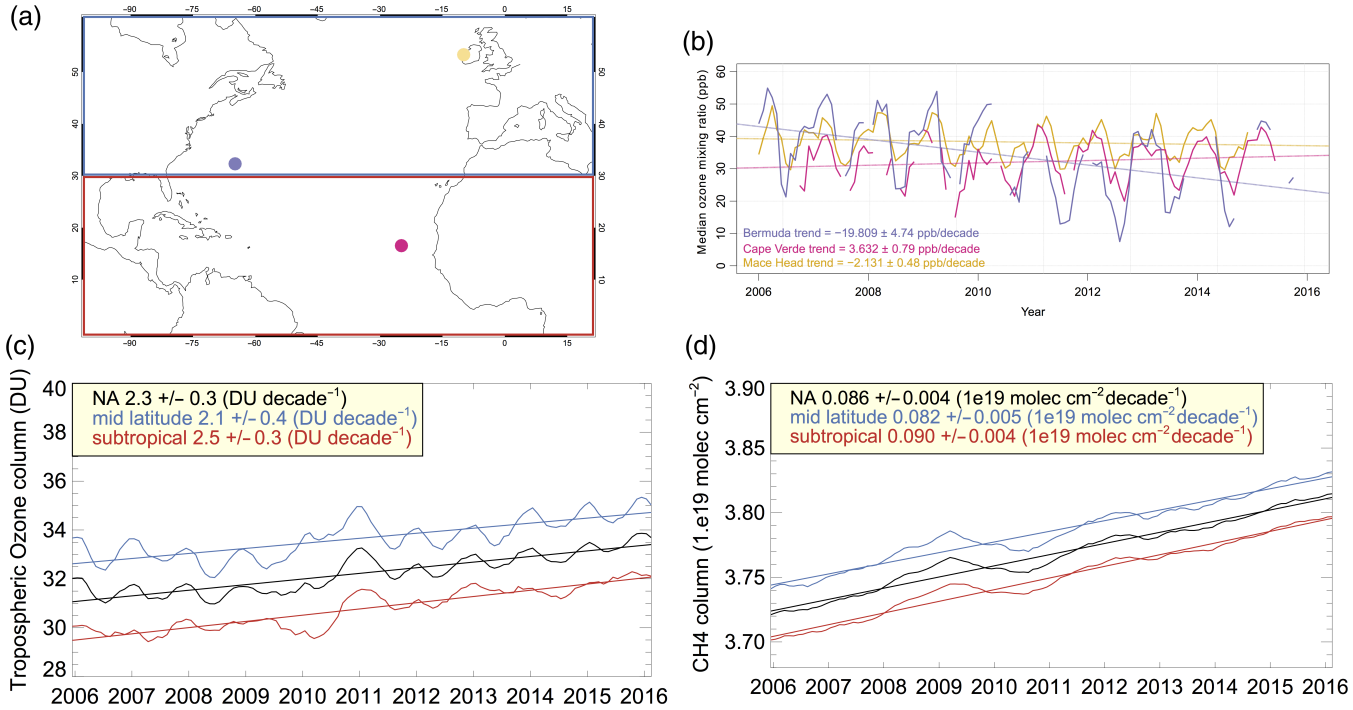

FIGURE 6 Time series from satellite and surface in situ measurements in the North Atlantic. Monthly median surface ozone mixing ratios (panel b) are shown for three long-term monitoring sites in the North Atlantic: Bermuda (64.87E; 32.31N), Cape Verde (24.87E; 16.54N), Mace Head (9.90E; 53.32N) (locations shown on panel a). Satellite trends (panels c and d) are calculated over the period 12/2005–2/2016 (123 months) for average values over three domains: North Atlantic (100°W–20°E; 0:60°N), mid-latitude (100°W–20°E; 30°–60°N), subtropical (100°W–20°E; 0:30°N). The curves plotted are 12 months running averages. Tropospheric ozone column trends from monthly OMI-MLS data; methane column trends from AIRS; surface in situ measurements from global atmospheric watch [Colour figure can be viewed at wileyonlinelibrary.com]

decade, while warming towards the tropics and the wintertime trend is again much larger than the summertime. Trends in the 700 hPa water mass mixing ratio (as measured by AIRS) are not distinguishable from the background variability over this time period. It is not clear how closely the trend patterns for water mass mixing ratio in both DJF and JJA (of around 0.0025 g/kg dry air) reflect the respective 700 hPa temperature trend patterns in the north Atlantic.

3 | RECENT CHANGES IN ATMOSPHERIC COMPOSITION

In this section, we concentrate on tropospheric ozone and methane; two important trace gases for which a recent satellite record exists. Ozone is produced in the troposphere through a complex interplay of reactions involving nitrogen oxides and organic and inorganic radicals (see, e.g., Monks *et al.* (2015) for more details). Because of its short lifetime in the troposphere (days to weeks), the largest ozone concentrations are often observed downwind but in close proximity to the sources of precursor gases. Methane, on the other hand, has a much longer lifetime in the troposphere (around 10 years) and is relatively well mixed. Changes in methane concentrations are generally thought to be mainly driven by changes in its emissions, which range from soils in natural wetlands through to fossil fuel production. More recently, changes in methane concentrations have also been attributed to changes in the concentration of the hydroxyl radical (OH), the main sink for methane, (Schaefer *et al.,* 2016; Prather and Holmes, 2017; Rigby *et al.,* 2017; Turner *et al.,* 2017). In this section, we document recent changes using surface observations and monthly mean gridded satellite data. The tropospheric ozone column was calculated from the Ozone Monitoring Instrument (OMI) and Microwave Limb Sounder (MLS) combination (OMI/MLS) as described in Ziemke *et al.* (2006) while methane total column was derived from the AIRS (Xiong *et al.,* 2008; Yurganov *et al.,* 2008).

3.1 | Time series of surface ozone at selected monitoring sites, tropospheric ozone column and total methane column

Figure 6 shows recent trends (ca. 2006–2016) of ozone and methane in the North Atlantic as measured at the surface and by satellite. Surface ozone shows a strong seasonal cycle across the North Atlantic, with a peak in spring and a minimum in the summer (see Figure 6b). Surface ozone at Bermuda has been decreasing significantly at a rate of 19.8 ppb/decade; this is likely due to the significant reduction in emissions of ozone precursors in the United States (Granier *et al.,* 2011). A smaller decrease is observed at Mace Head; in this case, the changes are harder to attribute and may

reflect local changes to the lifetime of ozone or the effect of large decreases in ozone precursors upwind of Mace Head. In contrast, surface ozone at Cape Verde has been increasing at a rate of 3.6 ppb/decade. This may be related to an increase in shipping, and hence ozone precursor emissions, a decrease in oceanic halogens, an important sink for ozone (Read *et al.,* 2008), or a general effect of the increases in methane, which acts as an important ozone precursor at the global scale (Young *et al.,* 2013).

Changes in tropospheric ozone column, Figure 6c, show a different picture, with a consistent increase across the North Atlantic. Several factors can contribute to trends in background tropospheric ozone including changes in emissions of ozone precursors, changes in temperature and solar radiation and long-range transport of ozone and its precursors. It has also been suggested that through El Niño/Southern Oscillation and the stratospheric Quasi-Biennial Oscillation, large-scale changes in climate may be affecting the transport of stratospheric rich ozone into the troposphere (Neu *et al.,* 2014), thereby increasing the tropospheric ozone burden.

The satellite retrievals of total column methane also show a strong, near linear, increase in methane over the North Atlantic in the last decade. This is consistent with our current understanding of global methane trends, for example, (Nisbet *et al.,* 2016). The methane trends are consistent across subregions of the North Atlantic, albeit the total column methane magnitude is smaller in the subtropics than in the mid-latitudes. A lower subtropical methane column is consistent with a shorter lifetime (due to higher concentrations of OH), weaker primary sources and stronger mixing into the stratosphere (through deep convection) in the tropics compared to mid-latitudes.

3.2 | Spatial and seasonal variability in observed trends

In this section, we analyse how trends in the observed columns of ozone and methane vary spatially and seasonally across the North Atlantic basin. Methane is a relatively long-lived gas which is generally well mixed at a regional scale and therefore very little spatial and seasonal variation in the North Atlantic trends is observed (not shown). On the other hand, ozone shows some interesting spatial variations with generally positive trends ranging between 0 and 15% per decade, depending on location. In winter (top panels of Figure 7), the spatial variability of ozone trends becomes larger with negative ozone trends over the Western part of the North Atlantic domain and very large positive trends over Central Europe and the Eastern part of the North Atlantic basin. In summer (middle panels in Figure 7) ozone shows a larger increase in the subtropical North Atlantic (STNA).

Observations from a small number of surface stations in the nineteenth century indicate that ozone concentrations

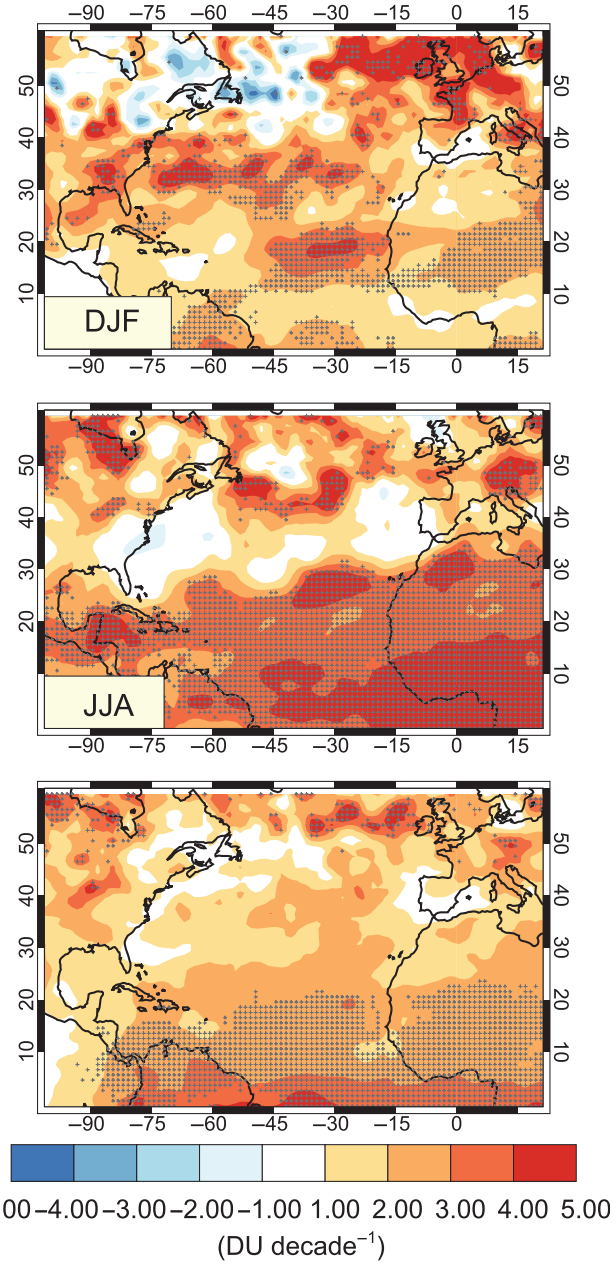

FIGURE 7 Decadal linear trends (ca. 2006–2016) calculated using seasonal (DJF [top] and JJA [middle]) and annual-mean (bottom) ozone tropospheric column. Trends are calculated over the period 12/2005–2/2016. The stippling indicates where trends are significant to the 95% confidence level, based on the standard error of the residuals (Wigley *et al*., 2006). Methane trends show little variation spatially and seasonally (not shown) [Colour figure can be viewed at wileyonlinelibrary.com]

have increased significantly since preindustrial times due to anthropogenic activities (Mickley *et al.,* 2001; Shindell *et al.,* 2006; Stevenson *et al.,* 2013). In developed countries, a recent reduction in the emissions of ozone precursors (Granier *et al.,* 2011) has helped decrease ozone levels and made an impact at the local and regional scale. However, different observational studies do not provide a consistent picture regarding the sign and magnitude of recent ozone trends at northern mid-latitudes (Cooper *et al.,* 2014; Parrish *et al.,* 2014; Ebojie *et al.,* 2016; Oetjen *et al.,* 2016). Our

study shows a generally small, but significant, positive trend over the North Atlantic for the period 2006–2016 (Figure 6c and Figure 7). The ozone increase seems to be larger and more robust for the STNA, and also for summer compared to winter. Despite looking at similar quantities, that is, tropospheric ozone column, our results and those of Ebojie *et al.* (2016) and Oetjen *et al.* (2016) all somewhat differ from each other. This is partly due to significant differences between the observing techniques and the different retrieval schemes applied. Similarly, the differences we identify between observed trends for surface and free tropospheric ozone are likely due to a decoupling between surface ozone (driven by local emission and sinks) and mid-tropospheric ozone (driven by large-scale transport and stratosphere-troposphere exchange (STE)).

3.3 | Impact of NAO on North Atlantic composition and possible effects on observed ozone trends

The positive phase of the NAO can increase the rate of transport of ozone and ozone precursors from North America to Europe. Ozone has a relatively short lifetime; therefore, faster transport across the North Atlantic can increase its abundance downwind of source regions. Changes in precipitation patterns (Scaife *et al.,* 2008) associated with the positive phase of the NAO (wetter than average Northern Europe and drier than average Southern Europe) can additionally affect ozone distribution by affecting the concentration of soluble ozone precursors. The NAO can also have an impact on modulating stratrop exchange (Simmonds *et al.,* 2013) which in turn can affect the regional ozone distribution in the North Atlantic.

Several studies have looked at intercontinental transport of tracers and pollutants and the role of the NAO in such transport pathways (Li *et al.,* 2002; Creilson *et al.,* 2003; Pausata *et al.,* 2012). Li *et al.* (2002) analysed modelled hourly surface ozone at Mace Head, for the period 1993–1997, and found it includes a significant fraction of North American ozone, around 10% on average throughout the year, and rising up to ~30% during transatlantic transport events. Creilson *et al.* (2003) analysed tropospheric ozone column (from TOMS/SBUV instruments) for the period 1979–2000 and found that, in some regions of the North Atlantic, tropospheric ozone is correlated to the NAO index. Similarly, Pausata *et al.* (2012) investigated the impact of NAO on ozone and found a positive correlation between the winter NAO index and ozone concentrations from surface stations in the United Kingdom and Northern Europe. They further suggested that summer NAO events could increase ozone concentrations over Europe, at a time when ozone levels are generally highest and could pose a threat to human health. As the NAO exerts a large influence on ozone transport over the North Atlantic, understanding future changes in the NAO and its influence on atmospheric composition is an important but little studied task (Bacer *et al.,* 2016).

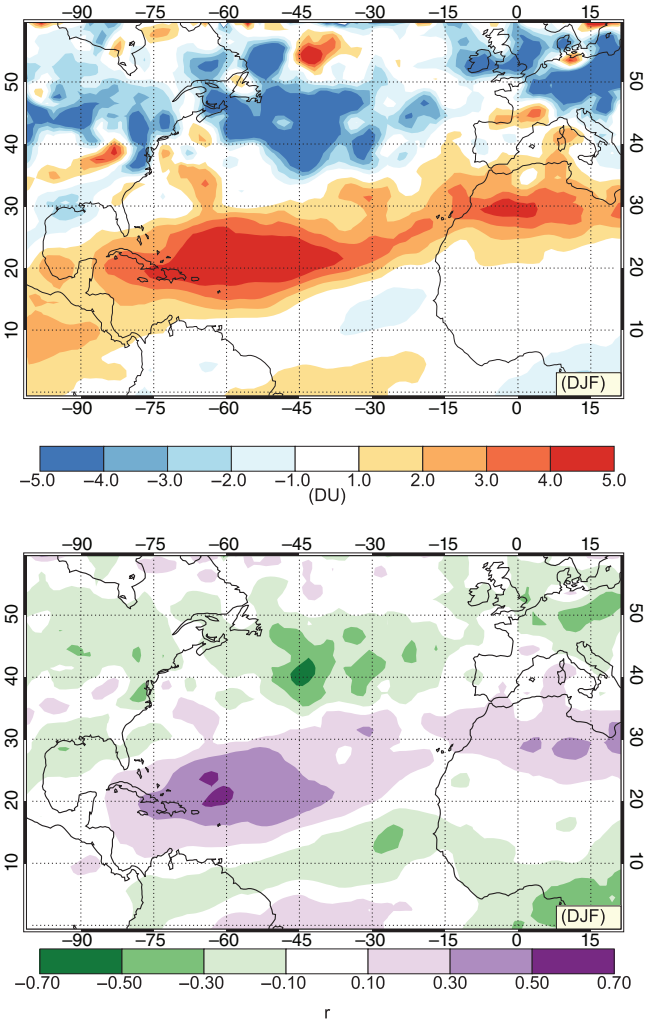

FIGURE 8 Impacts of NAO on tropospheric ozone column. Top panel shows difference in mean ozone tropospheric column between winter months with "high" and "low" NAO indices (high/low are defined as months between 12-2005 and 2-2016 with NAO index greater/smaller than +/−2). Bottom panel shows the correlation coefficient between tropospheric ozone column at each location and winter months NAO indices. NAO index is calculated as the difference between the normalized sea level pressure over Gibraltar and the normalized sea level pressure over SW Iceland (Jones *et al.,* 1997). Ozone data are detrended prior to the analysis [Colour figure can be viewed at wileyonlinelibrary.com]

We now focus on whether we can identify any influence of the winter NAO on the tropospheric ozone data used for this study and address whether changes in the NAO could partly explain observed or future ozone trends in the North Atlantic. Figure 8 (top panel) shows the difference in monthly mean tropospheric ozone column between winter months with "high" and "low" NAO indices. The top panel of Figure 8 suggests that the tropospheric ozone column decreases by up to 5–6 dobson units (DU) over large parts of North Europe, the United Kingdom and mid-latitude North Atlantic when the NAO is in its positive phase compared to when it is in its negative phase. Conversely, large areas of North Africa and STNA see an increase in tropospheric ozone column of 5–6 DU when the NAO is in its positive phase. This indicates a sizeable change in tropospheric ozone column over large areas of the North

Atlantic (up to ~15%) when the NAO switches between different phases. Furthermore, the bottom panel in Figure 8 shows that areas with the largest ozone changes are also strongly correlated with the winter NAO index. Although our findings and those of Pausata *et al*. (2012) disagree on the sign of the correlation over North Europe, the analysis of Pausata et al. focuses on surface ozone rather than tropospheric ozone column. The discrepancy in relationship between NAO and ozone can be attributed to the differences in the factors that control the behaviour of ozone at the surface and in the free troposphere, influencing the response of ozone to the NAO (Monks *et al.,* 2015).

In conclusion, different phases of the NAO can alter ozone concentrations at a regional level. Therefore, a future trend in the winter NAO index could have a large impact on ozone trends across different regions of the North Atlantic.

4 | RECENT CHANGES IN AEROSOLS, CLOUDS AND RADIATIVE FLUXES

Recent changes in aerosol, cloud and top of atmosphere radiative fluxes are assessed across the North Atlantic Ocean using several mature satellite observation products. These satellite observations span multiple decades and cover a wide range of spatial (from 1 km) and temporal scales (in daily intervals over 30 years in selected satellite missions). Top-of-atmosphere (ToA) shortwave and longwave fluxes are obtained from the Clouds and the Earth's Radiant Energy System Energy Balanced And Filled (CERES-EBAF version 2.8) product from the Terra satellite, and the European Space Agency (ESA) Climate Change Initiative Advanced Track Scanning Radiometer satellite derived fluxes using the Optimal Retrieval for Aerosol and Cloud (ORAC) algorithm. ORAC-ATSR retrieves top of atmosphere radiative fluxes at the 1-km pixel-scale imager resolution using BUGSrad, a correlated-k and Eddington approximation radiation model for retrieving broadband fluxes (Stephens *et al.,* 2001), in conjunction with the ORAC aerosol and cloud retrieval (Christensen *et al.,* 2016). Cloud and aerosol properties are analysed in MODerate Resolution Imaging Spectroradiometer (MODIS) standard collection six data and ATSR ORAC retrieval. Daytime data are averaged into monthly time intervals over 1° × 1° regions. MODIS/CERES provides data from the Terra satellite over the period from 2000 to present day. The ATSR satellite series contain two satellites the ATSR-2 which provides observations from 1995 to 2003 and AATSR which provided data from 2002 to 2012.

4.1 | Observed trends

The North Atlantic Ocean encompasses a variety of regional climates. Radiative fluxes across this region are strongly influenced by the mid-latitude storm track, dry subtropics where low-level clouds interact with offshore Saharan dust, and deep convective clouds (Harrison et al., 1990). Trends in the energy budget at the top of the atmosphere using 10 years (2006–2016) of CERES observations are displayed in Figure 9. Net *radiative* cooling (south of the Azores; box 1 in Figure 9c) and warming (in the West Atlantic, box 2 in Figure 9c) trends are evident [we use the term cooling to imply an increase in the net upward LW + southwest (SW) radiation]. The radiative changes in these regions are correlated (mostly) with the changes in cloud-cover fraction (influencing reflected sunlight and hence shortwave radiative cooling, Figure 9d) and/or cloud-top pressure (influencing longwave radiative emission, Figure 9e; box 2 region). Aerosols may also indirectly interact with these clouds causing subsequent changes in their optical properties that typically cause shortwave radiative cooling (Twomey, 1974), although this effect cannot be deduced from these data. Increases in aerosol loading are apparent from the positive trend in aerosol optical depth (AOD) in a zonal strip oriented off the African Saharan coast (Figure 9f). This increase is likely to be associated with dust aerosol from the African continent, which may have implications for cloud ice nucleation (e.g., Atkinson *et al.,* 2013; Welti *et al.,* 2017). The extent to which the increased aerosol loading off the coast of Africa is affecting the cloud properties demands further investigation. On the other hand, decreases in AOD occur off the east coast of the United States and Europe over the same period.

The East Atlantic box region (box 1) is related to an increase in the reflected shortwave radiative flux, which is associated with the large increase in reflective low-level clouds (Figure 10b,c), and longwave radiative cooling, due to the negative cloud top pressure trends (i.e., cloud-top height is increasing, Figure 9c). An evident seasonal cycle in cloud fraction is present in the East Atlantic with the maximum cloud fraction occurring in winter in both the standard MODIS and ATSR-ORAC retrieval (Figure 10b,c). In box 1, ATSR is found to retrieve a higher fraction of low-level clouds than MODIS although ATSR tends to underestimate the total cloud fraction relative to MODIS. This underestimation in ATSR is possibly due to weaker sensitivity using fewer channels than MODIS (Poulsen *et al.,* 2011).

In the West Atlantic (box 2), the positive net TOA flux trend corresponds to a negative trend in the outgoing longwave radiation, which is associated with a decrease in cloud to pressure. This could indicate an increase in cloud-top heights, and/or an increase in high-level clouds that emit less longwave radiation to space (i.e., trapping more heat in the troposphere). While smaller by comparison, we also observe a reduction in low-level clouds during this period. Combined with the increase in overall cloud fraction in this region seen in Figure 9d, this indicates an increase in mid- and high-altitude cloud fraction. A decrease in low-level cloud would give rise to radiative warming (when there is no overlying cloud). Therefore, both flux trends (shortwave and longwave) contribute to the substantial radiative warming trend in the West Atlantic region.

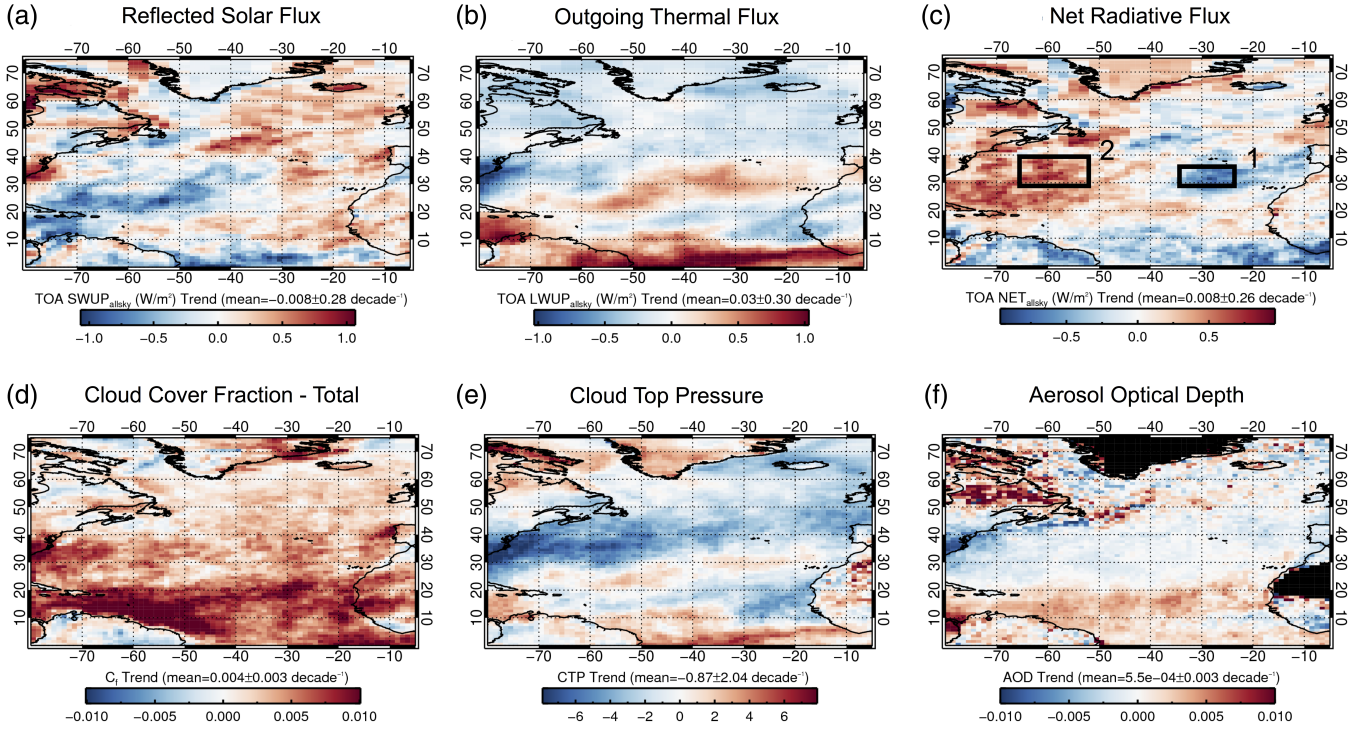

FIGURE 9 Trends in the anomalies computed from the monthly mean top of atmosphere (a) outgoing shortwave, (b) outgoing longwave, and (c) net radiative flux computed using All-sky monthly mean CERES-EBAF during the period 2006–2016 over the North Atlantic region (note positive is a net downwards flux in c). The MODIS MOD08_M3 product also displays (d) All-sky cloud cover fraction, (e) cloud top pressure and (f) AOD. Trends are computed using the period 2006–2016 over the North Atlantic region. Two boxes are displayed showing regions with substantial cooling (box 1 in the East Atlantic) and warming (box 2 in the West Atlantic). Mean trends of the anomalies are reported as a change per decade. Regions in black contain missing data [Colour figure can be viewed at wileyonlinelibrary.com]

Trends were also examined for individual seasons (not shown). During DJF, the net radiative flux trends are similar and slightly amplified compared to the annual flux trends; this is particularly notable for the very strong positive AOD trend off the coast of Saharan Africa. During JJA, the net radiative flux trends in the East Atlantic (i.e., box 1) reverse sign (i.e., they become positive) resulting in more energy absorption. This reversal in sign may be due to a decreasing cloud fraction trend during this season, possibly caused by decreasing aerosols.

4.2 | Discussion

Here, we have used mature satellite data products to examine the recent changes in aerosols, clouds and radiative fluxes across the North Atlantic Ocean and we have identified net radiative flux trends over the 2006–2016 period. Changes in cloud properties largely control the radiative flux responses. These changes may be caused by changes meteorological and/or atmospheric composition. For example, the regime switch from low-level to deeper-level clouds in the West Atlantic region (box 2) may be affected by changes in SST, atmospheric stability, aerosols, or possibly numerous other related factors that need to be explored in subsequent work with high-resolution models.

The NAO also affects SST and the thermodynamics that influence cloud formation. The NAO may also drive strong cloud radiative feedbacks as suggested by Yuan *et al.* (2016). For example, the positive phase of the NAO is associated with weaker trade winds and reduced dust outflow and a decrease in cloud top pressure off the coast of the Saharan desert, which results in further warming of the tropical North SST's. This dynamical feedback, as described in Yuan *et al.* (2016), is corroborated here by the correlation analysis with the NAO index (Figure 11a) and the top of atmosphere net cloud radiative effect (Figure 11b). The strong correlation pattern (regions have Pearson correlation coefficients >0.4) in the TOA radiative fluxes and increase in dust outflow over this period implies there may indeed be a strong connection between the NAO, cloud radiative effect, cloud fraction, and emission of dust aerosol (e.g., the trends in Figure 9c are highly correlated to the correlation trend with the NAO in Figure 11b). By including meteorological factors and comparing these trend results with regional-scale models, the process-scale interactions influencing cloud radiative feedbacks will advance our understanding of the North Atlantic Climate system.

5 | RECENT TRENDS IN OCEAN CIRCULATION AND PROPERTIES

The Subpolar North Atlantic (SPNA) and STNA are characterized by large wind-driven gyres which meet at circa 45°N, where the upper ocean Gulf Stream/North Atlantic

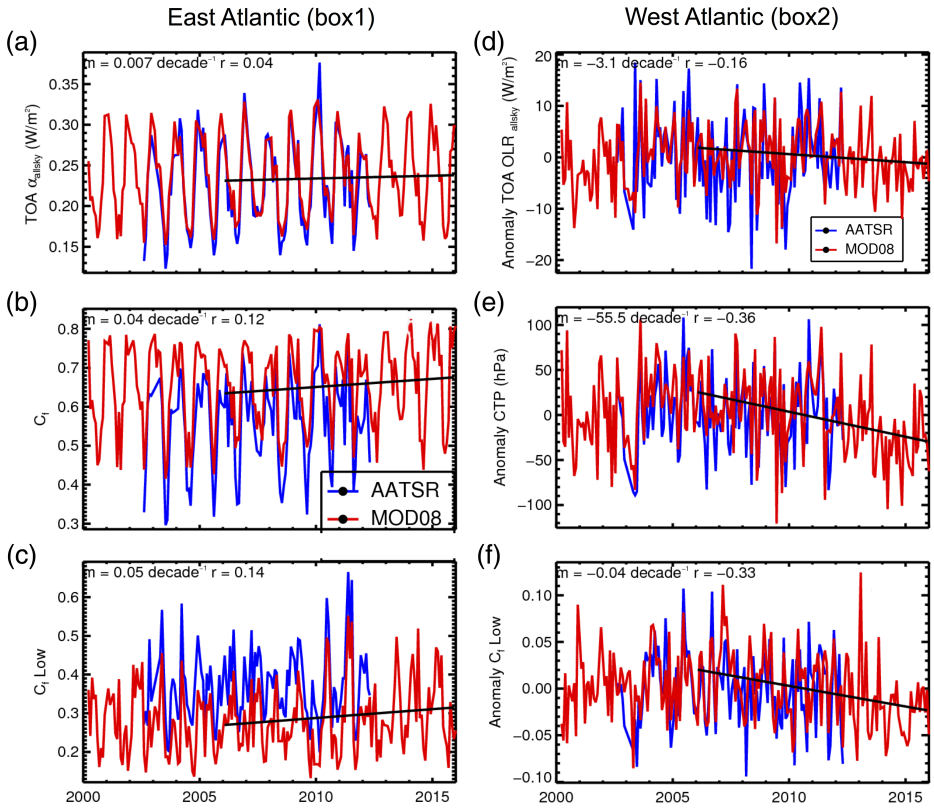

FIGURE 10 Monthly averages of (a) top of atmosphere All-sky albedo, (b) total cloud fraction and (c) low-level cloud fraction defined as a cloud top pressure greater than 500 hPa for the observations in the East Atlantic region (box 1). Monthly anomalies of (d) top of atmosphere outgoing longwave flux, (e) cloud top pressure and (f) low-level cloud fraction (for box 2). MODIS (red line) and AATSR (blue line) data sets are shown and the trend is computed over MODIS observations from 2006 to 2016. Anomalies (right panel only) are computed using the 2002–2012 period from independent retrievals from AATSR and MODIS observations. The slope (m) and correlation coefficient (*r*) are provided for each time series [Colour figure can be viewed at wileyonlinelibrary.com]

Current system feeds subtropical water into the eastern SPNA (see Figure 13g for schematic of North Atlantic Ocean Circulation). A warm net northward flow is balanced by returning colder intermediate (1,000–2,000 m) and deep layers (>2,000 m) concentrated in the deep western boundary currents: the basic vertical structure of the AMOC.

From 1996 to circa 2005, a range of indicators in the SPNA evolved in essentially the same way. For much of the record, the upper ocean trend was to higher sea level, higher SSTs and greater ocean heat content (see Figure 12). However, the period since 2006 has shown a different pattern and that of surface cooling and decreasing heat content above 1,000 m (Figure 14a,b). Some of the upper ocean and surface cooling can be explained by cold winters with high heat loss from the ocean to the atmosphere (Figure 13f) (Josey *et al.,* 2015; de Jong and de Steur, 2016; Duchez *et al.,*

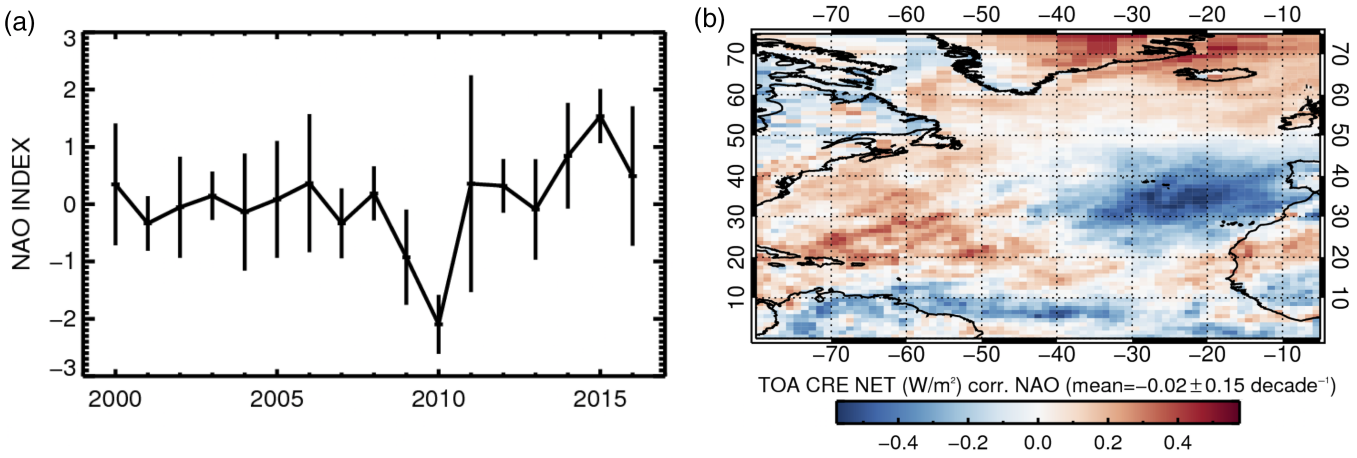

FIGURE 11 (a) NAO index averaged over DJF months (Hurrell, 1995) and (b) correlation of the observed cloud radiative effect (CERES) with the NAO index over the period from 2000 to 2016 [Colour figure can be viewed at wileyonlinelibrary.com]

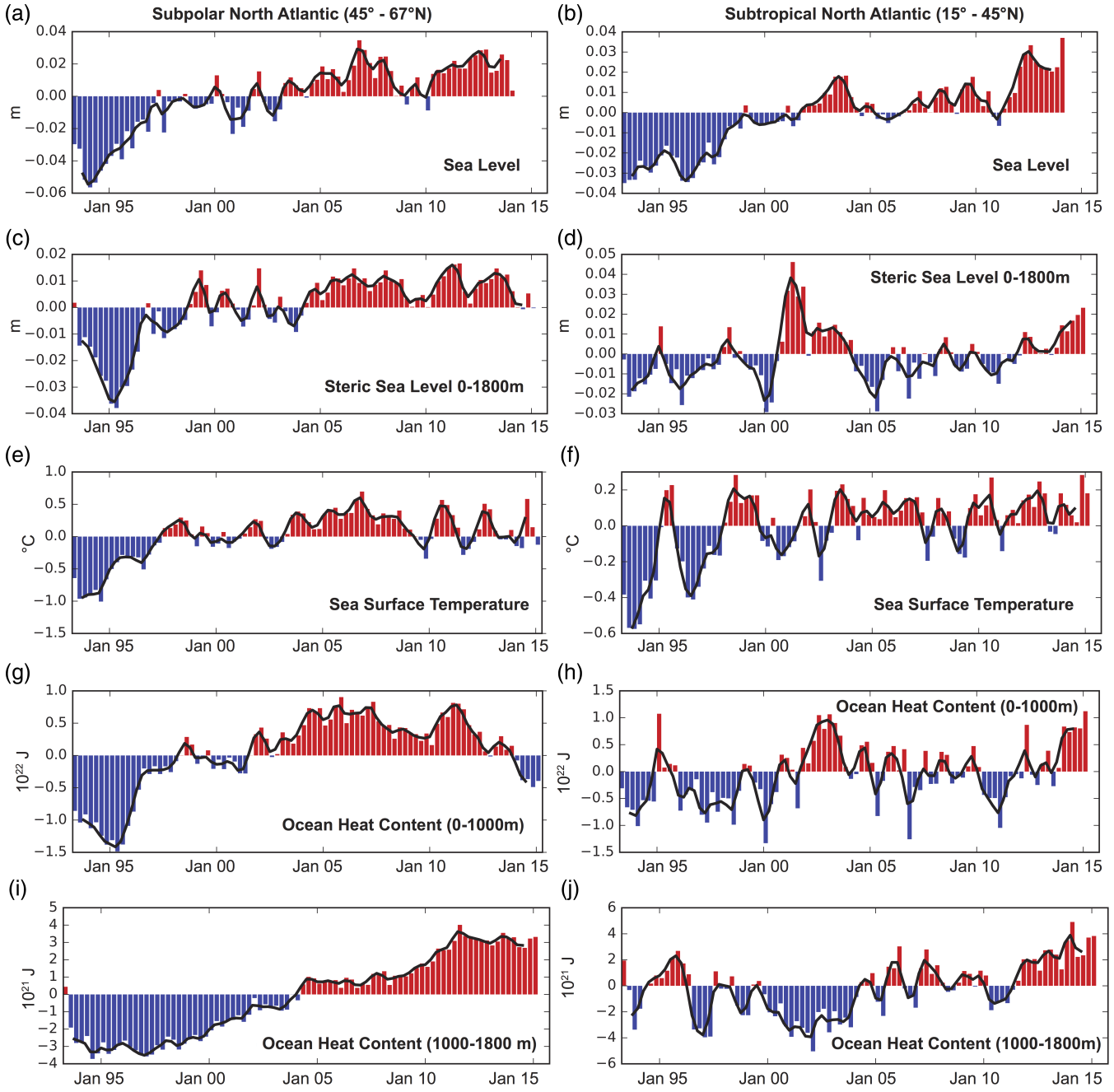

FIGURE 12 Time series of North Atlantic subpolar (left column) and subtropical (right column) sea level, SST and ocean heat content anomalies. (a,b) Sea level change (m), and (c,d) Steric sea level change (m), all anomalies from 1993 to 2014 mean seasonal means. (e,f) SST anomalies from the 1993 to 2014 seasonal means. (g,h) A 0–1,000 m ocean heat content anomaly from 1993 to 2015 seasonal mean and (i,j) Same except 1,000–1,800 m. Sea level and SST data are from the ESA-CCI project (Hollmann *et al.,* 2013; Merchant *et al.,* 2014; Ablain et al. 2015, 2017). Heat content anomalies derived from EN4 data sets (Good *et al.,* 2013) (www.metoffice.gov.uk/hadobs/en4/) [Colour figure can be viewed at wileyonlinelibrary.com]

2016; Grist *et al.,* 2016). Unusually, deep convection (to 1,600 m) was observed in the Labrador Sea in winter 2014/2015 (Yashayaev and Loder, 2016), though the convection has not yet reached the depths observed during the last extended period of deep convection (1987–1994, 2,100 m) when the heat content was lower than it is today. The occurrence of cold winters, heat loss and convective activity is strongly associated with the sign of the NAO index. The cold conditions in the mid-1990s in Figure 12 developed over two decades of increasingly positive NAO conditions (see Figure 1a,b), and the high heat loss in 2008, 2014 and 2015 were also under NAO positive conditions.

In the SPNA, heat loss to the atmosphere is replenished to a greater or lesser extent by the transport of heat in the upper ocean from the subtropics. This ocean heat transport is thought to be a dominant factor in setting multiyear patterns of SPNA upper ocean heat content (Robson *et al.,* 2012; Williams *et al.,* 2014). The mechanisms for ocean heat transport include the AMOC and the circulation of the gyres, and these may respond to different forcing on different time

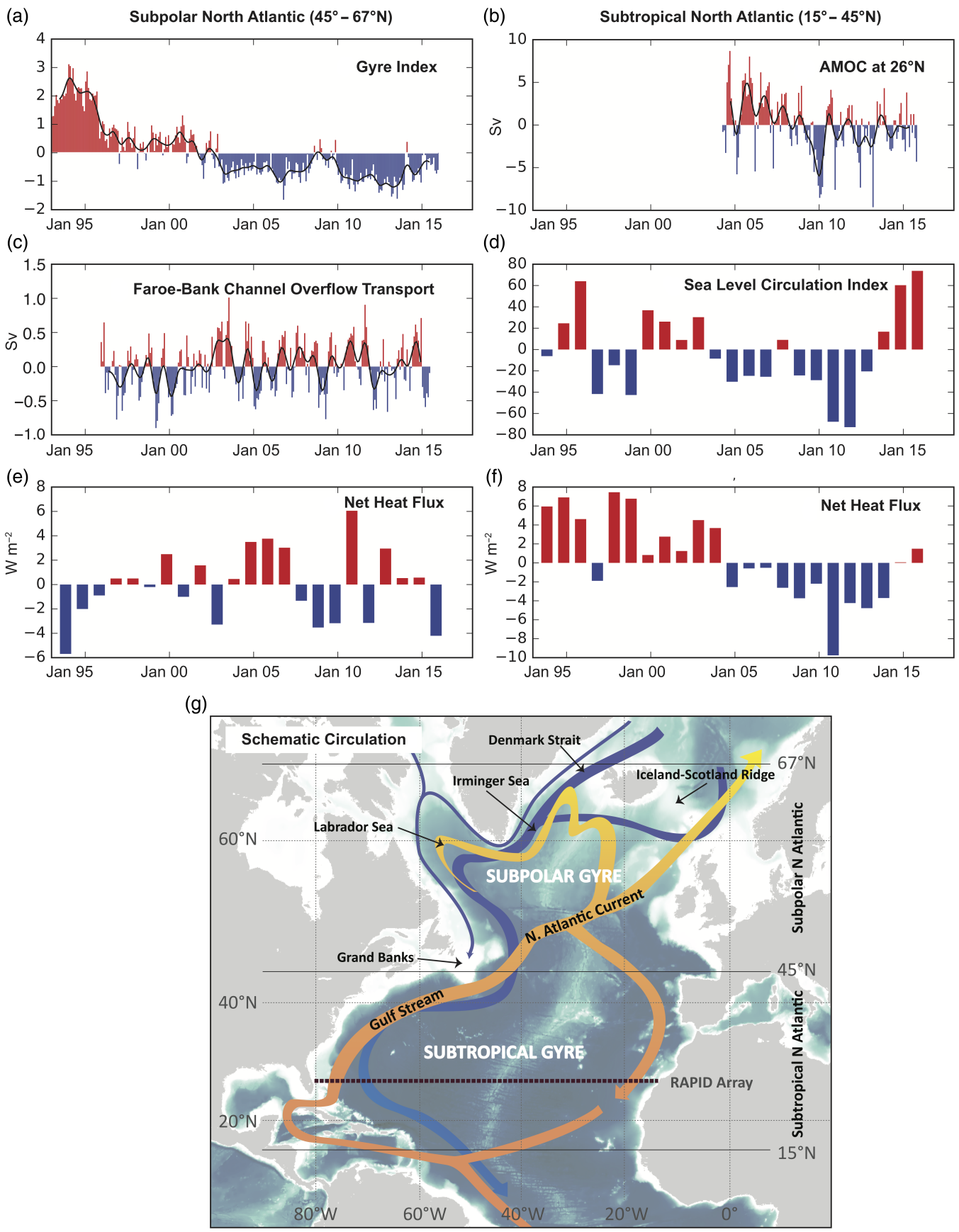

FIGURE 13 Time series of North Atlantic Ocean circulation and air-sea heat flux anomalies. (a) A subpolar gyre circulation index derived from ESA-CCI Sea level product (principle component of first EOF of SPNA Sea surface height). (b) The meridional overturning circulation observed at 26°N by the RAPID array (www.rapid.ac.uk). (c) The transport of overflow water at the Faroe Bank Channel (after Hansen *et al.*, 2016). (d) A subtropical-to-subpolar circulation index derived from sea-level gradient along the east coast of North America (after McCarthy et al., 2015). (e,f) Net heat flux derived from ERA-interim reanalysis data product. All anomalies are from 1993 to 2015 mean, or full time series length if shorter. (g) A schematic of North Atlantic Ocean circulation, and key regions [Colour figure can be viewed at wileyonlinelibrary.com]

scales. A measure of decadal changes in heat transport from the STNA to the SPNA is given in an index derived from the sea level gradient along the eastern U.S. coast (McCarthy et al., 2015a), Figure 13d). When a 7-year low-pass filter is applied, this index leads the rate of change of SPNA surface temperature trends by around 2 years (McCarthy et al., 2015a). The index is closely related to the NAO and matches the trend towards negative NAO from 2000 to 2011, reversing sharply in the previous few years in response to the shift to positive NAO. A measure of subpolar gyre heat transport is given by an index derived from sea surface height gradients across the region (Häkkinen and Rhines, 2004; Berx and Payne, 2016) (Figure 13a). Multi-year periods of decreasing index imply a slowing gyre circulation in association with decreasing wind stress curl, increased occurrences of atmospheric blocking events (Hakkinen *et al.,* 2011; Hanna *et al.,* 2016) which are linked to periods of warmer, more saline eastern SPNA. The decadal-scale trend in the index reflects the long-term change in basin-scale steric height (Foukal and Lozier, 2017).

SPNA sea level remains high despite the recent cooling (Figure 12a), even while the steric sea level contribution (from salinity and temperature) has decreased (Figure 12c). Some property changes are be density compensating and do not directly contribute to sea level changes (Mauritzen *et al.,* 2012; Desbruyères *et al.,* 2017). For most of the 1993–2015 periods, the steric sea level component follows a very similar pattern to the upper ocean heat content, though Figure 14 shows that changes in salinity oppose the thermosteric changes to some extent. The mass component of total sea level rise (i.e., from ice loss, or changes in land water storage) is clearly significant in the SPNA.

At intermediate depths (1,000–1,800 m), the SPNA is dominated by Labrador Sea Water (LSW). Formed in the Labrador and Irminger Seas by deep winter convection and freshened by mixing with Arctic-origin shallow outflows, the LSW spreads southward to form the upper part of the AMOC deep return flow. Since 1995, after the cessation of the last major deep convection period in the Labrador Sea, this layer has been steadily warming and increasing in salinity as it restratifies and mixes with warm, saline boundary currents (Lazier *et al.,* 2002), while elsewhere it also mixes with surrounding water types (Yashayaev *et al.,* 2007). This means that since 2006, the SPNA intermediate layer has been changing in an opposite sense to the upper layer. The 2014/2015 convection reached 1,600 m in the Labrador Sea (Yashayaev and Loder, 2016), but this localized event has apparently not yet impacted on the heat content averaged across the whole basin (Figure 12i).

The data coverage in the deepest SPNA layer of dense northern overflows (>2,000 m) is restricted to locations where repeated measurements are made from ships and moored instruments. We observe in the overflows a small increase in salinity from 1996 to 2015 at the Iceland-Scotland ridge, a slight cooling at the Denmark Strait, and remarkably steady volume transport at both (see Figure 13c) (Jochumsen *et al.,* 2012; Hansen *et al.,* 2016). By the time, the overflows reach the Labrador Sea they have increased in volume by entraining upper layer and intermediate water, and thus we observe a much larger increase in salinity and density in the Labrador Sea between 1996 and 2015 (Yashayaev and Loder, 2016).

The LSW and overflows exit the subpolar gyre west of the Grand Banks, becoming known as the upper and lower North Atlantic Deep Water (NADW). NADW enters the subtropical gyre in the "transition zone" (Buckley and Marshall, 2016) where it encounters the subtropical waters of the Gulf Stream extension. Some of the deep waters take interior pathways southwards (Bower *et al.,* 2009; Lozier *et al.,* 2013) but most form the deep western boundary current. By 30°N, the classical pattern of subtropical Atlantic circulation is established, with a horizontal gyre circulation in the top 1,000 m interacting with the large-scale overturning circulation (northwards in the top 1,000 m, southwards below 1,000 m) (Bryden and Imawaki, 2001). The balance of warm shallow waters moving northwards, with cold deep waters coming southward, leads to the largest heat transport of any ocean. Since 2004, the RAPID project has been measuring the AMOC at 26°N (McCarthy et al., 2015b).

Time scales of variability in the subtropical Atlantic differ from the SPNA. The SPNA shows a smoother, decadal-scale variability and the STNA shows much more interannual variability as it responds to local forcing as well as large-scale, longer term forcing (Bingham *et al.,* 2007). This is reflected in the time series of heat content, SST and sea-level change in the last 20 years also (Figure 12). While overall STNA sea level has risen in a similar manner to the SPNA (reflecting perhaps the global trend in sea level rise), the steric sea level, SST and upper ocean heat content anomaly show much more variable patterns in the STNA than the SPNA equivalents. Interannual timescale variability in the subtropics complicates the comparison between the SPNA and STNA but opposing patterns of variability are expected to be seen between the two gyres on decadal to multidecadal timescales due to opposing wind driven circulation changes (Williams *et al.,* 2014).

The measurements from the RAPID array can be used to understand these processes. Large and unexpected interannual variability was observed in the AMOC at 26°N in 2009 to 2010 (McCarthy *et al.,* 2012). The AMOC dropped in strength by 30% for a period of 18 months (Figure 13b). This was most likely wind initiated (Roberts *et al.,* 2013) and had the effect of cooling the subtropical ocean through ocean heat transport divergence (Cunningham *et al.,* 2013). However, a longer term weakening of the AMOC has also been ongoing. The AMOC had a strength of 18.5 Sv from 2004 to 2008 but only 15.5 Sv from 2009 to 2015 (updated

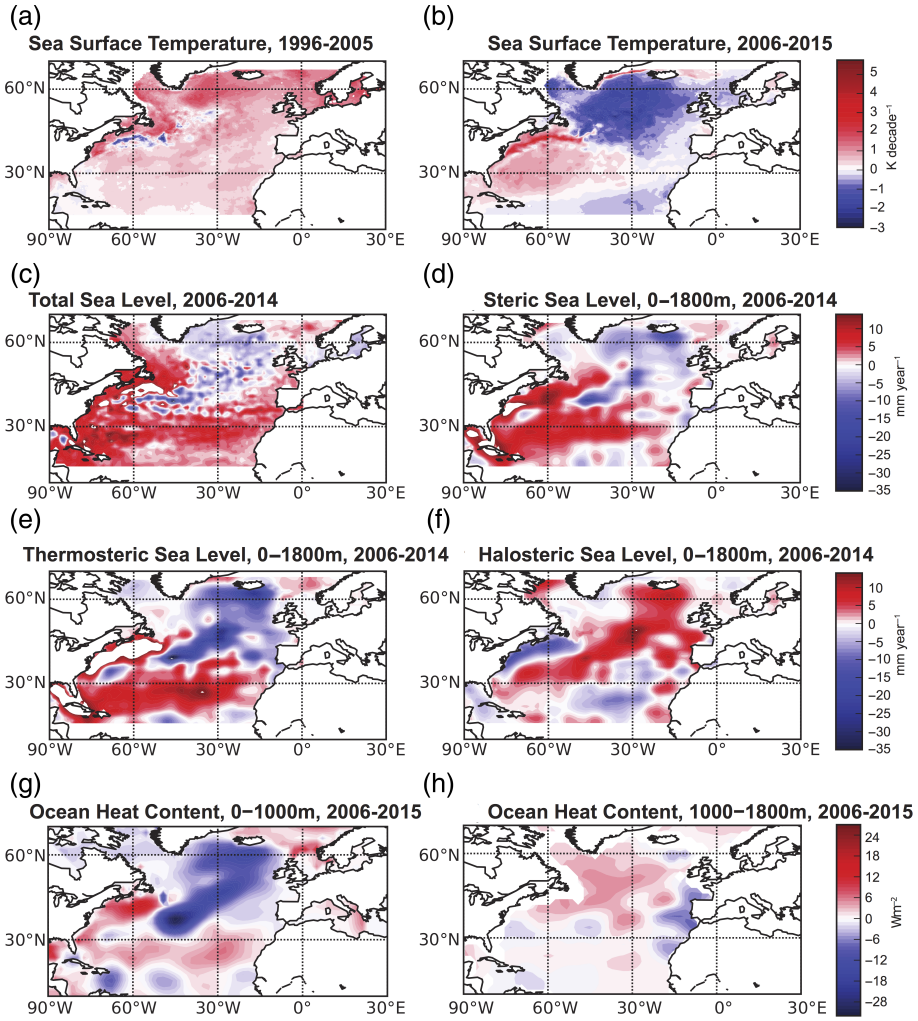

FIGURE 14 Recent decadal trends of key North Atlantic Ocean variables. (a) SST trend for 1996–2005. (b) SST trend for 2006–2015. (c) Sea level trend for 2006–2014. (d) Total steric sea level trend (0–1,800 m) for 2006–2014. (e) Thermosteric Sea level trend (0–1,800 m) for 2006–2014. (f) Halosteric Sea level trend (0–1,800 m) for 2006–2014. (g) Ocean heat content trend for 2006–2016 (0–1,000 m). (h) Ocean heat content trend for 2006–2016 (1,000–1,800 m). Sea level and SST data are from the ESA climate change initiative project. Heat content, steric, thermostreic and halosteric anomalies derived from EN4 data set [Colour figure can be viewed at wileyonlinelibrary.com]

from Smeed *et al.,* 2014). Changes in the transport of deep water masses had the largest influence on this 10-year decline. The decadal slowdown in overturning is likely to warm the subtropics and cool the subpolar North Atlantic (NA) as it leads to a reduction in heat exported from the subtopics to higher latitudes—a pattern that is consistent with the evolution of heat content in both gyres since 2010.

The pattern of large-scale cooling associated with a reduction in strength of the overturning circulation is linked, in climate models and reanalyses, to reduced densities in the deep Labrador Sea (in those studies meaning 1,000-2,500 m) (Robson *et al.,* 2014; Jackson *et al.,* 2016; Robson *et al.,* 2016). In observations, this depth range is called the upper NADW, which has its origins in the LSW that is observed to have multidecadal changes in density in the source region (Yashayaev and Loder, 2016). However, direct signatures of Labrador Sea density changes such as those described in (Ortega *et al.,* 2011) have yet to be seen at 26°N. Disentangling these (predominantly wind-driven) changes that cause the vertical displacement (or heave) of isopycnal surfaces from changes driven by source water changes is a key problem in understanding the LSW–AMOC link.

In observations at 26°N, the greatest changes in density and transport are in the lower NADW (LNADW, 3,000–5,000 m), which has origins in the dense overflows of the SPNA (Smeed *et al.,* 2014). To interpret, the slowdown in LNADW transport in the STNA as a consequence of changes in the overflows is an oversimplification. Indeed, as we have seen, the overflows have been remarkable constant in their volume transport over the last 20 years. At 26°N and throughout the STNA, in the depth range of NADW, density is higher on the western boundary than on the eastern boundary, defining the velocity shear pattern allowing for southwards flowing NADW. The density of the LNADW at 26°N has decreased on the western boundary since 2004, directly driving some of the weakening in the LNADW transports (Smeed *et al.,* 2014, see their Figure 6). The same pattern of deep density reduction is seen at 16°N (Frajka-Williams

et al., 2018). At 26°N, a large amount of the total change in the LNADW transport reduction since 2004 appears as a compensation to thermocline/gyre changes in order to balance mass across the section. This mass constraint has been independently verified, within an accuracy of approximately 1 Sv, in models (Hirschi and Marotzke, 2007), by bottom pressure recorder data (Kanzow *et al.,* 2007) and gravity satellite, GRACE, data (Landerer *et al.,* 2015). While undoubtedly a real signal, the changes in LNADW due to compensation are perhaps less interesting that those due to the change in density. Deep density changes are the mechanism by which the AMOC collapses in a range of CMIP5 models under future greenhouse gas emissions scenarios (McCarthy *et al.,* 2017) and perhaps offer the earliest hints of detectability of an AMOC collapse (Baehr *et al.,* 2007).

A notable change in the STNA in the last 10–20 years has been a southwards shift in the path of the Gulf Stream. This is most evident in patterns of sea level change (Figure 14c–e) but also in trends in SST and upper ocean heat content (Figure 14b,g). The Gulf Stream path is known to vary on multiannual and longer time scales. This variability is characterized by meridional shifts in the position of the Gulf Stream extension known as the Gulf Stream North Wall (GSNW). The relationship between the GSNW and the AMOC is disputed with some authors arguing that a northwards shift accompanies a strengthening AMOC (McCarthy et al., 2015a) and other authors arguing that a southwards shift accompanies a strengthening AMOC (Joyce and Zhang, 2010), with the former view being supported by the patterns observed in the last decade.

6 | CURRENT STATE AND RECENT CHANGES IN NORTH ATLANTIC SEA ICE AND THE GREENLAND ICE SHEET

This section summarizes the nature and drivers of recent changes to North Atlantic sea ice and the Greenland Ice Sheet. We first describe decadal variability in sea ice extent, regional ice concentration and sea ice volume. We then summarize the recent behaviour of the Greenland Ice Sheet, and the processes responsible for the ice sheet's evolution.

6.1 | Decadal variability of Arctic sea ice

Satellites have observed a decline in Arctic sea ice extent for all months since 1979 (Fetterer *et al.,* 2017; Perovich *et al.,* 2017), coincident with abrupt global and Arctic warming over the last 30 years (Hartmann *et al.,* 1990). Over that period, the surface temperature in the Arctic increased at almost twice the global average rate—a phenomena known as Arctic amplification. As sea ice and snow retreat, surface albedo decreases and more solar radiation is absorbed by the Arctic Ocean (Curry *et al.,* 1995) providing a positive feedback on surface temperature. The surface albedo feedback is often cited as the main contributor to the observed Arctic amplification (Serreze and Barry, 2005; Screen and Simmonds, 2010; Taylor *et al.,* 2013). However, increased cloud cover (Winton, 2006), and an ocean–atmosphere heat exchange as sea ice diminishes (Lindsay and Zhang, 2005; Serreze and Barry, 2005) also likely contributed. The satellite-observed decline in ice extent is strongest in September, when Arctic sea ice extent reaches its annual minimum. September sea ice extent decreased by 13% decade^{-1} from 1979 to 2016, resulting in a record minimum ice extent of 3.41 million km^2 on 16 September, 2012 (Fetterer *et al.,* 2017). The 10 lowest minimum Arctic sea ice extents on satellite record have all occurred since 2005.

Further insight into changes in Arctic-wide and regional sea ice cover can be gained from mapping recent annual anomalies in ice concentration relative to decadal means (Figure 15). In spring (March/April; towards the end of the sea ice growth season) 2016, there was little difference in the concentration of sea ice in the central Arctic compared with the 2005–2016 mean. However, there were significant differences in springtime ice concentration in the more southerly regions that have a predominantly seasonal, first year ice cover. Within the Atlantic sector (defined as the area encompassing the Greenland Sea, Iceland Sea, Barents Sea, Kara Sea, White Sea, Labrador Sea, and Gulf of St Lawrence/Nova Scotia peninsula—see Figure S2), the 2016 ice concentration was anomalously low in the Greenland, Iceland and Barents Seas but higher in the western Labrador Sea and Gulf of St Lawrence, and along the Nova Scotia peninsula. In autumn (October/November; the period following the annual minimum sea ice extent) 2016, Arctic-wide sea ice concentration was ~15% lower than the 2005–2016 mean, coincident with the decline observed in Arctic-wide sea ice extent. The greatest anomalous lows occurred in the Iceland and Kara Seas, which are regions that fall within the Atlantic sector and have seasonally varying sea ice cover.

Sea ice concentration has also exhibited large interannual variability in recent years. Within the Atlantic Sector, and indeed the wider Arctic, 2016 was an unusual year. At the end of March 2016, sea ice extent was below average in most of the seasonal regions, most notably in the Barents and Kara seas, but not the Labrador Sea. These variations were associated with anomalously warm conditions over the Arctic Ocean, driven by a pattern of above-average sea level pressures centred over the ocean north of Alaska, and below-average pressures over the Atlantic side of the Arctic (NOAA, 2017). In addition, the Barents and Kara seas were experiencing an influx of warm Atlantic waters (NSIDC, 2016a). The autumn of 2016 was associated with unusually slow growth of sea ice following the annual minimum extent, and in the Kara Sea, it has been suggested that the slow ice growth was due to above average SSTs for the time of year (NSIDC, 2016b).

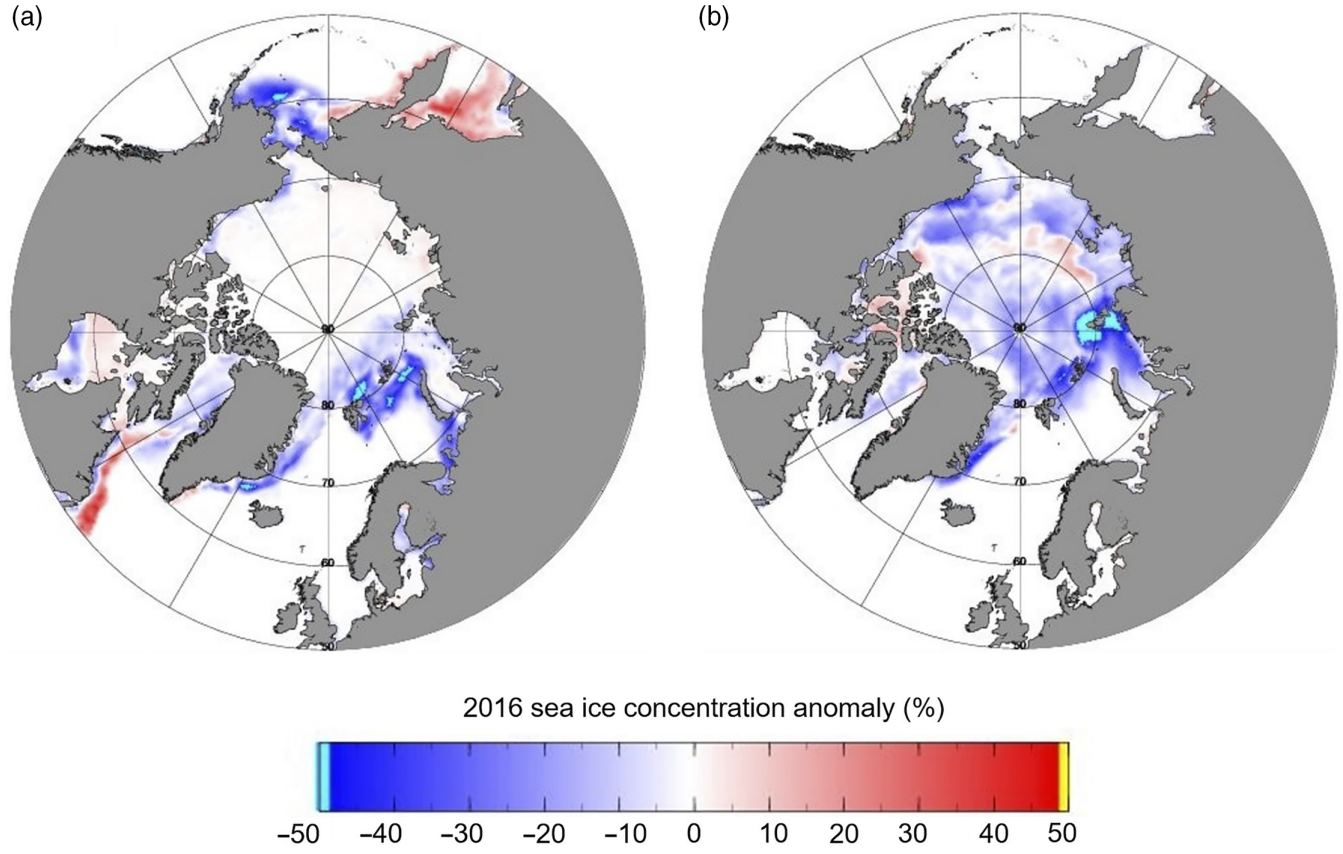

FIGURE 15 Arctic Sea ice concentration anomaly in 2016, relative to the 2005–2016 mean, for (a) spring (March/April) and (b) autumn (October/November), from PIOMAS. Regions with a mean sea ice concentration less than 5% are not shown, and the extent is masked for 2016 [Colour figure can be viewed at wileyonlinelibrary.com]

6.2 | Importance of Arctic sea ice thickness and volume observations

Arctic-wide observations of sea ice concentration have provided insight into decadal-scale changes in the ice cover. However, to fully understand regional and global impacts of these changes, long-term accurate estimates of total ice volume are required. Sea ice thickness and volume estimates can be obtained from some models, such as the Pan-Arctic Ice-Ocean Modelling and Assimilation System (PIOMAS; Zhang and Rothrock, 2003). From an observational perspective, the ESA's CryoSat-2 satellite (Wingham *et al.,* 2006) provides unparalleled coverage of the Arctic Ocean up to 88°N since 2010. CryoSat-2 data have been used to produce the first observational estimates of sea ice thickness and volume across the entire Northern Hemisphere over the sea ice growth season, before melt ponds begin to form on the ice (Tilling *et al.,* 2015; Tilling *et al.,* 2016).

Since 1980, PIOMAS shows a decline in Arctic sea ice volume for autumn of 16% decade^{-1} and a decline in spring volume of 8% decade^{-1} (Figure 16). Since 2005, the decline in autumn volume has increased to 25% decade^{-1} whereas the decline in spring volume has remained more stable at 9% decade^{-1}. Over the CryoSat-2 period alone ,there have been clear seasonal and interannual variations in the volume of Northern Hemisphere sea ice cover. For example, between 2010 and 2016, the large (349–468 km^3 year^{-1}) interannual fluctuations in ice volume (Figure 16) were two to three times greater than the variability that occurred in the central Arctic between 2003 and 2008 (115–275 km^3 year^{-1})—the only other period for which satellite observations of Arctic sea ice volume exist (Kwok *et al.,* 2009). For the CryoSat-2 period, the Atlantic sector contributed 9 and 14% to the total autumn and spring sea ice

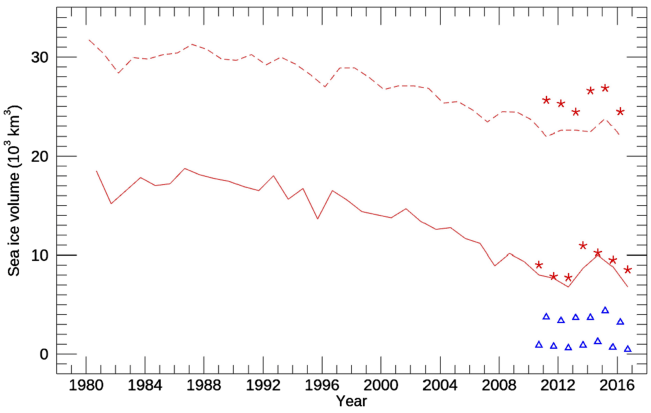

FIGURE 16 Time series of PIOMAS model Arctic Sea ice volume for autumn 1980–2015 (solid line) and spring 1980–2016 (dashed line). CryoSat-2 volume estimates are plotted for autumn (October/November) 2010–2014 and spring (March/April) 2011–2014, Arctic-wide (red stars) and within the Atlantic sector (blue triangles) [Colour figure can be viewed at wileyonlinelibrary.com]

volume, respectively. Total autumn sea ice volume declined by 14% (1,279 km^3) between 2010 and 2012, increased by 41% (3,184 km^3) in 2013, and then decreased by 22% (2,629 km^3) between 2013 and 2016. The peak autumn volume in 2013 was associated with the retention of thick ice in the multi-year ice region north of Greenland and Ellesmere Island coincident with a ~5% drop in the number of days on which melting occurred over summer. The sharp increase in sea ice volume after just one cool summer demonstrates the ability of Arctic sea ice to respond rapidly to a changing environment (Tilling *et al.,* 2015).

6.3 | Recent changes in the mass of the Greenland ice sheet

Since the early 1990s, mass loss from the Greenland Ice Sheet has contributed approximately 10% of the observed global mean sea level rise (Vaughan *et al.,* 2013). During this period, the ice imbalance has progressively increased with time (Rignot *et al.,* 2011; Shepherd *et al.,* 2012), from 34 ± 40 Gt year^{-1} between 1992 and 2001, to 215 ± 59 Gt year^{-1} between 2002 and 2011 (Vaughan *et al.,* 2013), and to 269 ± 51 Gt year^{-1} between 2011 and 2014. The latter rate corresponds to an annual contribution of 0.74 ± 0.14 mm year^{-1} to global mean sea level (McMillan *et al.,* 2016), ~25% of the total observed budget (Hanna *et al.,* 2013b). Regionally, Greenland's South West has experienced the greatest loss of ice (Figure 17), contributing ~40% of the total ice sheet imbalance between 2011 and 2014 (McMillan *et al.,* 2016). In contrast, the North East sector contributed ~10% of ice losses, with the remainder split almost equally between the South East and North West sectors (Figure 17).

Satellite, airborne and field observations show that ice loss has been predominantly focussed upon ice margin regions and marine terminating outlet glaciers (Krabill *et al.,* 2004; Thomas *et al.,* 2006; Rignot *et al.,* 2010; Enderlin *et al.,* 2014; Joughin *et al.,* 2014), which are sensitive to warming at their atmospheric and ocean interfaces. Inland, within the cooler, slow-flowing interior, and particularly at more southerly latitudes, snowfall driven mass accumulation occurred throughout the 1990s and up to 2005 (Thomas *et al.,* 2006). However, since 2005 inland snowfall, and associated mass gains, appear to have diminished (Kuipers Munneke *et al.,* 2015). Over shorter, interannual timescales, Greenland's mass balance has fluctuated considerably (Figure 17). In 2012, for example, a record mass deficit of 439 ± 62 Gt was recorded, only to be followed in 2013 by losses of 116 ± 65 Gt in 2013, which were approximately half the 2000–2011 mean (McMillan *et al.,* 2016). At the finer scale of individual glacier systems, the spatial and temporal pattern of variability is also complex, with glacier response to changes in ocean (Holland *et al.,* 2008) and atmospheric (Fettweis *et al.,* 2011; van den Broeke *et al.,* 2017) forcing being modulated by both glacier geometry and setting.

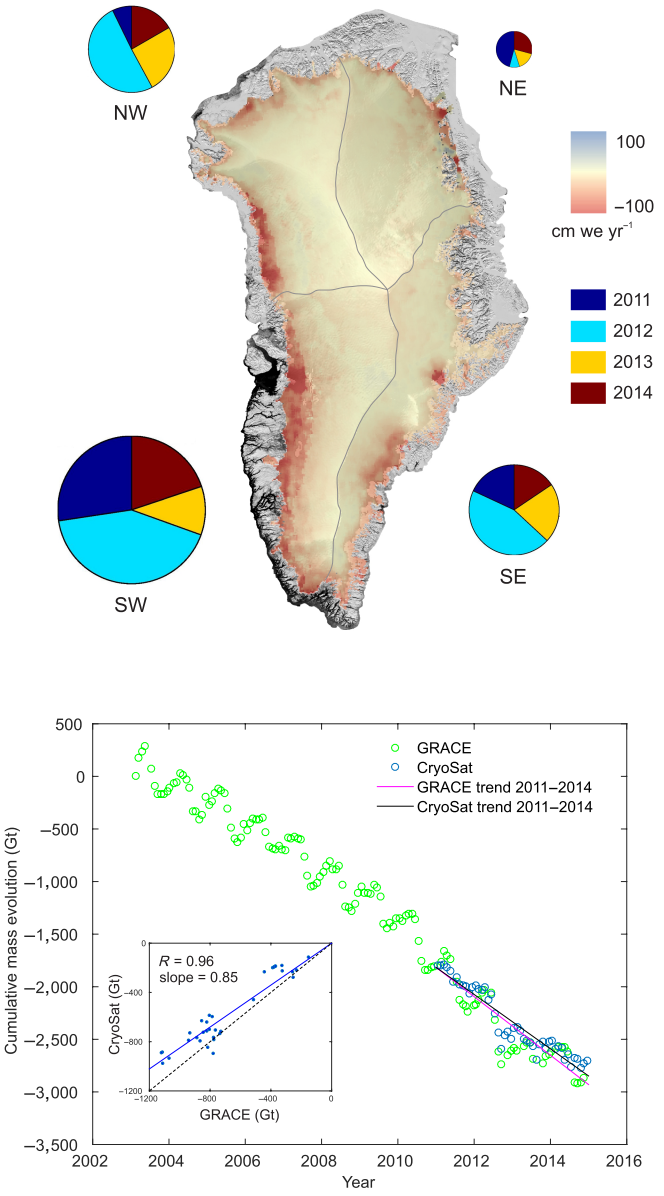

FIGURE 17 Top panel. Rate of mass change of the Greenland ice sheet between January 2011 and December 2014. For each of the SW, southeast (SE), NE and northwest (NW) sectors, the colour wheel indicates the proportion of mass lost in each year, with the radius scaled according to the magnitude of the total losses. The boundaries between the four sectors are shown in grey. Bottom panel. Monthly evolution in ice sheet mass since 2003 from GRACE gravimetry (green) and since 2011 from CryoSat-2 altimetry and firn modelling (blue). The CryoSat-2 time series has been referenced to the GRACE data at the start of 2011. The inset shows the correspondence between the GRACE and CryoSat-2 monthly estimates of mass evolution since 2011 (solid blue dots), together with a linear regression (solid blue line), the regression slope and the Pearson correlation coefficient, *R*. The dashed line indicates equivalence, although the GRACE results include, additionally, mass changes of peripheral ice caps and unglaciated regions (McMillan *et al.,* 2016) [Colour figure can be viewed at wileyonlinelibrary.com]

6.4 | Drivers of recent changes in the mass of the Greenland ice sheet

Recent fluctuations in Greenland Ice Sheet mass have been driven by two processes; changing surface mass balance and variable glacier flow. Between 2000 and 2008 ice loss was

due, in almost equal amounts, to decreased surface mass balance and increased ice discharge (van den Broeke *et al.,* 2009; Fettweis *et al.,* 2017; Noël *et al.,* 2018). These changes were driven by a combination of warmer summer temperatures (Hanna *et al.,* 2008b; Fettweis *et al.,* 2013), and glacier flow acceleration across much of the South East and North West sectors (Enderlin *et al.,* 2014).

Since 2008, several exceptionally warm summers have produced episodes of widespread surface melt (Nghiem *et al.,* 2012; Fettweis *et al.,* 2013), which has been particularly intense along the western margin of the ice sheet (Hanna *et al.,* 2012). In particular, 2012 and 2015 have been notable because of the extensive summer melting that occurred across the entire (2012) and northern (2015) sectors of the ice sheet (Nghiem *et al.,* 2012; Tedesco *et al.,* 2016). Intense, short-term melt events such as these can have a large impact on annual variability in ice sheet melting, and have been linked to the advection of warmer southerly air over the ice sheet driven by persistent high pressure systems associated with a strong negative phase of the NAO (see Figure 1c) and a high Greenland Blocking Index (Hanna *et al.,* 2014). In contrast, 2013 saw low-pressure and low-temperature conditions, coinciding with the most positive summertime NAO recorded in the past 20 years (see Figure 1c), and unusually low ice mass loss in that year. Together, these contrasting years illustrate the recent sensitivity of Greenland's annual mass imbalance to large-scale modes of atmospheric variability, with intense melt events lasting only a few months capable of making relatively large contributions to the overall mass deficit.

7 | SYNTHESIS AND DISCUSSION

This report has brought together an unprecedented range of evidence about recent changes in the North Atlantic Climate System. It documents trends in atmospheric circulation and composition, in ocean circulation and properties, and in the cryosphere, with a primary focus on the period since 2000 and especially since 2005. Focussing on the period since 2005, some of the major trends identified and discussed include:

- An increase in the speed of the North Atlantic jet stream in winter (Figure 2a) associated with an increase in sea level pressure across the mid-latitude Atlantic and a decrease in the northeast (NE) Atlantic (Figure 3b).
- Increases in ozone and methane (Figures 6 and 7).
- Increases in net absorbed radiation in the mid-latitude western Atlantic, which correlates with an increase in the abundance of high-level clouds and a reduction in low-level clouds (Figure 10).
- Cooling of SSTs in the subpolar gyre, concomitant with increases in the western subtropical gyre, and a decline in the Atlantic overturning circulation (Figures 13 and 14).
- A decline in Atlantic sector Arctic sea-ice and increased rates of melting of the Greenland Ice Sheet (Figures 16 and 17).

The report raises many questions about the significance and causes of the various trends, and—implicitly—the extent to which they may continue in future, or change. The report is structured around the different components of the North Atlantic Climate System but a fundamental point is that the trends in these different components are not independent. There are many exchange processes that link the different variables, and understanding the relative importance of different processes is an important challenge. Some examples of the linkage questions raised by this report are as follows:

- What have been the roles of atmospheric circulation and composition in driving the trends in ocean circulation and properties?
- To what extent have the changes in atmospheric circulation been influenced by the changes in SST?
- What has been the role of atmospheric circulation, including the NAO, in shaping the trends in ozone and methane?
- To what extent have the changes in clouds and net absorbed radiation been a factor in the (similarly located) warming of SST in the western subtropical gyre? And to what extent have the SST trends influenced the clouds?
- What has been the role of atmosphere and ocean circulation in driving the trends observed in Atlantic sector sea ice and Greenland Ice Sheet mass?

Maintaining and expanding the observational capacity in the North Atlantic and continuing in-depth process-based analysis of observations and models is crucial to unravel these linkages.

ACKNOWLEDGEMENTS

This review article was written with support of the NERC North Atlantic Climate System: integrated Study (ACSIS) project. The authors would like to thank the three anonymous reviewers for their useful suggestions.

ORCID

Jon Robson http://orcid.org/0000-0002-3467-018X
Adam Scaife http://orcid.org/0000-0002-5189-7538

REFERENCES

Atkinson, J.D., Murray, B.J., Woodhouse, M.T., Whale, T.F., Baustian, K.J., Carslaw, K.S., Dobbie, S., O'Sullivan, D. and Malkin, T.L. (2013) The

importance of feldspar for ice nucleation by mineral dust in mixed-phase clouds. *Nature*, 498, 355–358. https://doi.org/10.1038/nature12278.

Ba, J., Keenlyside, N.S., Latif, M., Park, W., Ding, H., Lohmann, K., Mignot, J., Menary, M., Otterå, O.H., Wouters, B., Melia, D.S.Y., Oka, A., Bellucci, A. and Volodin, E. (2014) A multi-model comparison of Atlantic multidecadal variability. *Climate Dynamics*, 43, 2333–2348. https://doi.org/10.1007/s00382-014-2056-1.

Bacer, S., Christoudias, T. and Pozzer, A. (2016) Projection of North Atlantic Oscillation and its effect on tracer transport. *Atmospheric Chemistry and Physics*, 16, 15581–15592. https://doi.org/10.5194/acp-16-15581-2016.

Baehr, J., Haak, H., Alderson, S., Cunningham, S.A., Jungclaus, J.H. and Marotzke, J. (2007) Timely detection of changes in the meridional overturning circulation at 26°N in the Atlantic. *Journal of Climate*, 20, 5827–5841. https://doi.org/10.1175/2007JCLI1686.1.

Bell, C.J., Gray, L.J., Charlton-Perez, A.J., Joshi, M.M. and Scaife, A.A. (2009) Stratospheric communication of El Niño teleconnections to European winter. *Journal of Climate*, 22, 4083–4096. https://doi.org/10.1175/2009JCLI2717.1.

Berx, B. and Payne, M.R. (2016) The sub-polar gyre index—a community data set for application in fisheries and environment research. *Earth System Science Data*, 9, 259–266. https://doi.org/10.5194/essd-2016-53.

Biastoch, A., Böning, C.W. and Lutjeharms, J.R.E. (2008) Agulhas leakage dynamics affects decadal variability in Atlantic overturning circulation. *Nature*, 456, 489–492. https://doi.org/10.1038/nature07426.

Bingham, R.J., Hughes, C.W., Roussenov, V. and Williams, R.G. (2007) Meridional coherence of the North Atlantic meridional overturning circulation: meridional coherence of Atlantic MOC. *Geophysical Research Letters*, 34, L23606. https://doi.org/10.1029/2007GL031731.

Blaker, A.T., Hirschi, J.J.-M., McCarthy, G., Sinha, B., Taws, S., Marsh, R., Coward, A. and de Cuevas, B. (2015) Historical analogues of the recent extreme minima observed in the Atlantic meridional overturning circulation at 26 N. *Climate Dynamics*, 44, 457–473.

Booth, B.B.B., Dunstone, N.J., Halloran, P.R., Andrews, T. and Bellouin, N. (2012) Aerosols implicated as a prime driver of twentieth-century North Atlantic climate variability. *Nature*, 484, 228–232. https://doi.org/10.1038/nature10946.

Bower, A.S., Lozier, M.S., Gary, S.F. and Böning, C.W. (2009) Interior pathways of the North Atlantic meridional overturning circulation. *Nature*, 459, 243–247. https://doi.org/10.1038/nature07979.

Bryden, H.L. and Imawaki, S. (2001) Chapter 6.1 Ocean heat transport. Int. Geophys. *Ocean Circulation and Climate*, 77, 455–474. https://doi.org/10.1016/S0074-6142(01)80134-0.

Buckley, M.W. and Marshall, J. (2016) Observations, inferences, and mechanisms of the Atlantic meridional overturning circulation: a review. *Reviews of Geophysics*, 54, 2015RG000493. https://doi.org/10.1002/2015RG000493.

Cattiaux, J., Vautard, R., Cassou, C., Yiou, P., Masson-Delmotte, V. and Codron, F. (2010) Winter 2010 in Europe: a cold extreme in a warming climate. *Geophysical Research Letters*, 37, L20704. https://doi.org/10.1029/2010GL044613.

Cheng, L., Trenberth, K.E., Fasullo, J., Boyer, T., Abraham, J. and Zhu, J. (2017) Improved estimates of ocean heat content from 1960 to 2015. *Science Advances*, 3, e1601545. https://doi.org/10.1126/sciadv.1601545.

Christensen, M.C., Poulsen, C., McGarragh, G. and Grainger, R. (2016). Algorithm theoretical basis document (ATMD) of the community code for CLimate (CC4CL) broadband radiative flux retrieval (CC4CL-TOAFLUX) module, Version 1.0 (Phase 2 ESA cloud_cci report for cloud option #4).

Clement, A., Bellomo, K., Murphy, L.N., Cane, M.A., Mauritsen, T., Rädel, G. and Stevens, B. (2015) The Atlantic multidecadal oscillation without a role for ocean circulation. *Science*, 350, 320–324. https://doi.org/10.1126/science.aab3980.

Cooper, O.R., Parrish, D.D., Ziemke, J., Balashov, N.V., Cupeiro, M., Galbally, I.E., Gilge, S., Horowitz, L., Jensen, N.R., Lamarque, J.-F., Naik, V., Oltmans, S.J., Schwab, J., Shindell, D.T., Thompson, A.M., Thouret, V., Wang, Y. and Zbinden, R.M. (2014) Global distribution and trends of tropospheric ozone: an observation-based review. *Elementa Science of the Anthropocence*, 2, 000029. https://doi.org/10.12952/journal.elementa.000029.

Creilson, J.K., Fishman, J. and Wozniak, A.E. (2003) Intercontinental transport of tropospheric ozone: a study of its seasonal variability across the North Atlantic utilizing tropospheric ozone residuals and its relationship to the North Atlantic Oscillation. *Atmospheric Chemistry and Physics*, 3, 2053–2066. https://doi.org/10.5194/acp-3-2053-2003.

Cropper, T., Hanna, E., Valente, M.A. and Jónsson, T. (2015) A daily Azores-Iceland North Atlantic Oscillation index back to 1850. *Geoscience Data Journal*, 2, 12–24. https://doi.org/10.1002/gdj3.23.

Cunningham, S.A., Roberts, C.D., Frajka-Williams, E., Johns, W.E., Hobbs, W., Palmer, M.D., Rayner, D., Smeed, D.A. and McCarthy, G. (2013) Atlantic meridional overturning circulation slowdown cooled the subtropical ocean. *Geophysical Research Letters*, 40, 6202–6207. https://doi.org/10.1002/2013GL058464.

Curry, J.A., Schramm, J.L. and Ebert, E.E. (1995) Sea ice-albedo climate feedback mechanism. *Journal of Climate*, 8, 240–247. https://doi.org/10.1175/1520-0442(1995)008<0240:SIACFM>2.0.CO;2.

de Jong, M.F. and de Steur, L. (2016) Strong winter cooling over the Irminger Sea in winter 2014-2015, exceptional deep convection, and the emergence of anomalously low SST. *Geophysical Research Letters*, 43, 7106–7113. https://doi.org/10.1002/2016GL069596.

Dee, D.P., Uppala, S.M., Simmons, A.J., Berrisford, P., Poli, P., Kobayashi, S., Andrae, U., Balmaseda, M.A., Balsamo, G., Bauer, P., Bechtold, P., Beljaars, A.C.M., van de Berg, L., Bidlot, J., Bormann, N., Delsol, C., Dragani, R., Fuentes, M., Geer, A.J., Haimberger, L., Healy, S.B., Hersbach, H., Hólm, E.V., Isaksen, L., Kållberg, P., Köhler, M., Matricardi, M., McNally, A.P., Monge-Sanz, B.M., Morcrette, J.-J., Park, B.-K., Peubey, C., de Rosnay, P., Tavolato, C., Thépaut, J.-N. and Vitart, F. (2011) The ERA-interim reanalysis: configuration and performance of the data assimilation system. *Quarterly Journal of the Royal Meteorological Society*, 137, 553–597. https://doi.org/10.1002/qj.828.

Delworth, T.L. and Zeng, F. (2016) The impact of the North Atlantic oscillation on climate through its influence on the Atlantic meridional overturning circulation. *Journal of Climate*, 29, 941–962. https://doi.org/10.1175/JCLI-D-15-0396.1.

Desbruyères, D., McDonagh, E.L., King, B.A. and Thierry, V. (2017) Global and full-Depth Ocean temperature trends during the early twenty-first century from Argo and repeat hydrography. *Journal of Climate*, 30, 1985–1997. https://doi.org/10.1175/JCLI-D-16-0396.1.

Deser, C., Alexander, M.A., Xie, S.-P. and Phillips, A.S. (2010) Sea surface temperature variability: patterns and mechanisms. *Annual Review of Marine Science*, 2, 115–143. https://doi.org/10.1146/annurev-marine-120408-151453.

Driscoll, S., Bozzo, A., Gray, L.J., Robock, A. and Stenchikov, G. (2012) Coupled Model Intercomparison Project 5 (CMIP5) simulations of climate following volcanic eruptions. *Journal of Geophysical Research: Atmospheres*, 117, D17105. https://doi.org/10.1029/2012JD017607.

Duchez, A., Frajka-Williams, E., Josey, S.A., Evans, D.G., Grist, J.P., Marsh, R., McCarthy, G.D., Sinha, B., Berry, D.I. and Hirschi, J.J.-M. (2016) Drivers of exceptionally cold North Atlantic Ocean temperatures and their link to the 2015 European heat wave. *Environmental Research Letters*, 11, 074004. https://doi.org/10.1088/1748-9326/11/7/074004.

Ebojie, F., Burrows, J.P., Gebhardt, C., Ladstätter-Weißenmayer, A., von Savigny, C., Rozanov, A., Weber, M. and Bovensmann, H. (2016) Global tropospheric ozone variations from 2003 to 2011 as seen by SCIAMACHY. *Atmospheric Chemistry and Physics*, 16, 417–436. https://doi.org/10.5194/acp-16-417-2016.

Eden, C. and Willebrand, J. (2001) Mechanism of interannual to decadal variability of the North Atlantic circulation. *Journal of Climate*, 14, 2266–2280. https://doi.org/10.1175/1520-0442(2001)014<2266:MOITDV>2.0.CO;2.

Enderlin, E.M., Howat, I.M., Jeong, S., Noh, M.-J., van Angelen, J.H. and van den Broeke, M.R. (2014) An improved mass budget for the Greenland ice sheet. *Geophysical Research Letters*, 41, 866–872. https://doi.org/10.1002/2013GL059010.

Fereday, D.R., Maidens, A., Arribas, A., Scaife, A.A. and Knight, J.R. (2012) Seasonal forecasts of northern hemisphere winter 2009/10. *Environmental Research Letters*, 7, 034031. https://doi.org/10.1088/1748-9326/7/3/034031.

Fetterer, F., Knowles, K., Meier, W., Savoie, M. and Windnagel, A. K. (2017). Sea Ice Index, Version 3. https://doi.org/10.7265/N5K072F8

Fettweis, X., Box, J.E., Agosta, C., Amory, C., Kittel, C., Lang, C., van As, D., Machguth, H. and Gallée, H. (2017) Reconstructions of the 1900–2015 Greenland ice sheet surface mass balance using the regional climate MAR model. *The Cryosphere*, 11, 1015–1033. https://doi.org/10.5194/tc-11-1015-2017.

Fettweis, X., Hanna, E., Lang, C., Belleflamme, A., Erpicum, M. and Gallée, H. (2013) Brief communication: "Important role of the mid-tropospheric

atmospheric circulation in the recent surface melt increase over the Greenland ice sheet". *The Cryosphere*, 7, 241–248. https://doi.org/10.5194/tc-7-241-2013.

Fettweis, X., Mabille, G., Erpicum, M., Nicolay, S. and den Broeke, M.V. (2011) The 1958–2009 Greenland ice sheet surface melt and the mid-tropospheric atmospheric circulation. *Climate Dynamics*, 36, 139–159. https://doi.org/10.1007/s00382-010-0772-8.

Foukal, N.P. and Lozier, M.S. (2017) Assessing variability in the size and strength of the north Atlantic subpolar gyre: north Atlantic subpolar gyre variability. *Journal of Geophysical Research, Oceans*, 122, 6295–6308. https://doi.org/10.1002/2017JC012798.

Frajka-Williams, E., Lankhorst, M., Koelling, J. and Send, U. (2018) Coherent circulation changes in the Deep North Atlantic from 16°N and 26°N transport arrays. *Journal of Geophysical Research: Oceans*, 123, 3427–3443. https://doi.org/10.1029/2018JC013949.

Gastineau, G., D'Andrea, F. and Frankignoul, C. (2013) Atmospheric response to the North Atlantic Ocean variability on seasonal to decadal time scales. *Climate Dynamics*, 40, 2311–2330. https://doi.org/10.1007/s00382-012-1333-0.

Gastineau, G. and Frankignoul, C. (2014) Influence of the North Atlantic SST variability on the atmospheric circulation during the twentieth century. *Journal of Climate*, 28, 1396–1416. https://doi.org/10.1175/JCLI-D-14-00424.1.

Good, S.A., Martin, M.J. and Rayner, N.A. (2013) EN4: quality controlled ocean temperature and salinity profiles and monthly objective analyses with uncertainty estimates. *Journal of Geophysical Research, Oceans*, 118, 6704–6716. https://doi.org/10.1002/2013JC009067.

Granier, C., Bessagnet, B., Bond, T., D'Angiola, A., Denier van der Gon, H., Frost, G.J., Heil, A., Kaiser, J.W., Kinne, S., Klimont, Z., Kloster, S., Lamarque, J.-F., Liousse, C., Masui, T., Meleux, F., Mieville, A., Ohara, T., Raut, J.-C., Riahi, K., Schultz, M.G., Smith, S.J., Thompson, A., van Aardenne, J., van der Werf, G.R. and van Vuuren, D.P. (2011) Evolution of anthropogenic and biomass burning emissions of air pollutants at global and regional scales during the 1980–2010 period. *Climatic Change*, 109, 163–190. https://doi.org/10.1007/s10584-011-0154-1.

Gray, L.J., Beer, J., Geller, M., Haigh, J.D., Lockwood, M., Matthes, K., Cubasch, U., Fleitmann, D., Harrison, G., Hood, L., others, 2010. Solar influences on climate. *Reviews of Geophysics*, 48, RG4001. https://doi.org/10.1029/2009RG000282.

Gray, L.J., Scaife, A.A., Mitchell, D.M., Osprey, S., Ineson, S., Hardiman, S., Butchart, N., Knight, J., Sutton, R. and Kodera, K. (2013) A lagged response to the 11 year solar cycle in observed winter Atlantic/European weather patterns. *Journal of Geophysical Research: Atmospheres*, 118, 13–405. https://doi.org/10.1002/2013JD020062.

Gray, L.J., Woollings, T.J., Andrews, M. and Knight, J. (2016) Eleven-year solar cycle signal in the NAO and Atlantic/European blocking: 11-year solar cycle in NAO and Atlantic/European blocking. *Quarterly Journal of the Royal Meteorological Society*, 142, 1890–1903. https://doi.org/10.1002/qj.2782.

Grist, J.P., Josey, S.A., Jacobs, Z.L., Marsh, R., Sinha, B. and Van Sebille, E. (2016) Extreme air–sea interaction over the North Atlantic subpolar gyre during the winter of 2013–2014 and its sub-surface legacy. *Climate Dynamics*, 46, 4027–4045. https://doi.org/10.1007/s00382-015-2819-3.

Häkkinen, S. and Rhines, P.B. (2004) Decline of subpolar North Atlantic circulation during the 1990s. *Science*, 304, 555–559. https://doi.org/10.1126/science.1094917.

Hakkinen, S., Rhines, P.B. and Worthen, D.L. (2011) Atmospheric blocking and Atlantic Multidecadal Ocean variability. *Science*, 334, 655–659. https://doi.org/10.1126/science.1205683.

Hanna, E., Cappelen, J., Allan, R., Jónsson, T., Le Blancq, F., Lillington, T. and Hickey, K. (2008a) New insights into north European and North Atlantic surface pressure variability, storminess, and related climatic change since 1830. *Journal of Climate*, 21, 6739–6766. https://doi.org/10.1175/2008JCLI2296.1.

Hanna, E., Cropper, T.E., Hall, R.J. and Cappelen, J. (2016) Greenland blocking index 1851-2015: a regional climate change signal: Greenland blocking index 1851-2015. *International Journal of Climatology*, 36, 4847–4861. https://doi.org/10.1002/joc.4673.

Hanna, E., Cropper, T.E., Jones, P.D., Scaife, A.A. and Allan, R. (2015) Recent seasonal asymmetric changes in the NAO (a marked summer decline and increased winter variability) and associated changes in the AO and Greenland blocking index. *International Journal of Climatology*, 35, 2540–2554. https://doi.org/10.1002/joc.4157.

Hanna, E., Fettweis, X., Mernild, S.H., Cappelen, J., Ribergaard, M.H., Shuman, C.A., Steffen, K., Wood, L. and Mote, T.L. (2014) Atmospheric and oceanic climate forcing of the exceptional Greenland ice sheet surface melt in summer 2012. *International Journal of Climatology*, 34, 1022–1037. https://doi.org/10.1002/joc.3743.

Hanna, E., Huybrechts, P., Steffen, K., Cappelen, J., Huff, R., Shuman, C., Irvine-Fynn, T., Wise, S. and Griffiths, M. (2008b) Increased runoff from melt from the Greenland ice sheet: a response to global warming. *Journal of Climate*, 21, 331–341. https://doi.org/10.1175/2007JCLI1964.1.

Hanna, E., Jones, J.M., Cappelen, J., Mernild, S.H., Wood, L., Steffen, K. and Huybrechts, P. (2013a) The influence of North Atlantic atmospheric and oceanic forcing effects on 1900-2010 Greenland summer climate and ice melt/runoff. *International Journal of Climatology*, 33, 862–880. https://doi.org/10.1002/joc.3475.

Hanna, E., Mernild, S.H., Cappelen, J. and Steffen, K. (2012) Recent warming in Greenland in a long-term instrumental (1881–2012) climatic context: I. Evaluation of surface air temperature records. *Environmental Research Letters*, 7, 045404. https://doi.org/10.1088/1748-9326/7/4/045404.

Hanna, E., Navarro, F.J., Pattyn, F., Domingues, C.M., Fettweis, X., Ivins, E.R., Nicholls, R.J., Ritz, C., Smith, B., Tulaczyk, S., Whitehouse, P.L. and Zwally, H.J. (2013b) Ice-sheet mass balance and climate change. *Nature*, 498, 51–59. https://doi.org/10.1038/nature12238.

Hansen, B., Húsgarð Larsen, K.M., Hátún, H. and Østerhus, S. (2016) A stable Faroe Bank Channel overflow 1995–2015. *Ocean Science*, 12, 1205–1220. https://doi.org/10.5194/os-12-1205-2016.

Harrison, E.F., Minnis, P., Barkstrom, B.R., Ramanathan, V., Cess, R.D. and Gibson, G.G. (1990) Seasonal variation of cloud radiative forcing derived from the Earth Radiation Budget Experiment. *Journal of Geophysical Research*, 95 (D11), 18687–18703. https://doi.org/10.1029/JD095iD11p18687.

Hartmann, D.L., Klein-Tank, A.M.G., Rusticucci, M., Alexander, L.V., Brönnimann, S., Charabi, Y., Dentener, F.J., Dlugokencky, E.J., Easterling, D.R., Kaplan, A., Soden, B.J., Thorne, P.W., Wild, M. and Zhai, P.M. (2013) Observations: Atmosphere and surface. In: Stocker, T.F., Qin, D., Plattner, G.K., et al. (Eds.) *The Physical Science Basis. Contribution of Working Group I to the Fifth Assessment Report of the Intergovernmental Panel on Climate Change*. Cambridge, UK: Cambridge University Press, pp. 159–254.

Hátún, H., Payne, M.R., Beaugrand, G., Reid, P.C., Sandø, A.B., Drange, H., Hansen, B., Jacobsen, J.A. and Bloch, D. (2009) Large bio-geographical shifts in the North-Eastern Atlantic Ocean: from the subpolar gyre, via plankton, to blue whiting and pilot whales. *Progress in Oceanography*, 80, 149–162. https://doi.org/10.1016/j.pocean.2009.03.001.

Hewitt, H.T., Copsey, D., Culverwell, I.D., Harris, C.M., Hill, R.S.R., Keen, A. B., McLaren, A.J. and Hunke, E.C. (2011) Design and implementation of the infrastructure of HadGEM3: the next-generation Met Office climate modelling system. *Geoscientific Model Development*, 4, 223–253. https://doi.org/10.5194/gmd-4-223-2011.

Hirschi, J. and Marotzke, J. (2007) Reconstructing the meridional overturning circulation from boundary densities and the zonal wind stress. *Journal of Physical Oceanography*, 37, 743–763. https://doi.org/10.1175/JPO3019.1.

Hoerling, M.P., Hurrell, J.W., Xu, T., Bates, G.T. and Phillips, A.S. (2004) Twentieth Century North Atlantic Climate Change. Part II: Understanding the effect of Indian Ocean warming. *Climate Dynamics*, 23, 391–405. https://doi.org/10.1007/s00382-004-0433-x.

Holland, D.M., Thomas, R.H., de Young, B., Ribergaard, M.H. and Lyberth, B. (2008) Acceleration of Jakobshavn Isbræ triggered by warm subsurface ocean waters. *Nature Geoscience*, 1, 659–664. https://doi.org/10.1038/ngeo316.

Hollmann, R., Merchant, C.J., Saunders, R., Downy, C., Buchwitz, M., Cazenave, A., Chuvieco, E., Defourny, P., de Leeuw, G., Forsberg, R., Holzer-Popp, T., Paul, F., Sandven, S., Sathyendranath, S., van Roozendael, M. and Wagner, W. (2013) The ESA climate change initiative: satellite data Records for Essential Climate Variables. *Bulletin of the American Meteorological Society*, 94, 1541–1552. https://doi.org/10.1175/BAMS-D-11-00254.1.

Huntingford, C., Marsh, T., Scaife, A.A., Kendon, E.J., Hannaford, J., Kay, A. L., Lockwood, M., Prudhomme, C., Reynard, N.S., Parry, S., Lowe, J.A., Screen, J.A., Ward, H.C., Roberts, M., Stott, P.A., Bell, V.A., Bailey, M., Jenkins, A., Legg, T., Otto, F.E.L., Massey, N., Schaller, N., Slingo, J. and Allen, M.R. (2014) Potential influences on the United Kingdom's floods of

winter 2013/14. *Nature Climate Change*, 4, 769–777. https://doi.org/10.1038/nclimate2314.

Hurrell, J.W. (1995) Decadal trends in the North Atlantic oscillation: regional temperatures and precipitation. *Science*, 269, 676–679. https://doi.org/10.1126/science.269.5224.676.

Hurrell, J.W., Kushnir, Y., Ottersen, G. and Visbeck, M. (2003) An overview of the North Atlantic Oscillation. In: Hurrell, J.W., Kushnir, Y., Ottersen, G. and Visbeck, M. (Eds.) *Geophysical Monograph Series*. Washington, DC: American Geophysical Union, pp. 1–35. https://doi.org/10.1029/134GM01.

Ineson, S., Scaife, A.A., Knight, J.R., Manners, J.C., Dunstone, N.J., Gray, L.J. and Haigh, J.D. (2011) Solar forcing of winter climate variability in the Northern Hemisphere. *Nature Geoscience*, 4, 753–757. https://doi.org/10.1038/ngeo1282.

Jackson, L.C., Peterson, K.A., Roberts, C.D. and Wood, R.A. (2016) Recent slowing of Atlantic overturning circulation as a recovery from earlier strengthening. *Nature Geoscience*, 9, 518–522. https://doi.org/10.1038/ngeo2715.

Jochumsen, K., Quadfasel, D., Valdimarsson, H. and Jónsson, S. (2012) Variability of the Denmark Strait overflow: Moored time series from 1996–2011: Denmark strait overflow. *Journal of Geophysical Research: Oceans*, 117, C12003. https://doi.org/10.1029/2012JC008244.

Jones, P.D., Jonsson, T. and Wheeler, D. (1997) Extension to the North Atlantic oscillation using early instrumental pressure observations from Gibraltar and south-West Iceland. *International Journal of Climatology*, 17, 1433–1450. https://doi.org/10.1002/(SICI)1097-0088(19971115)17:13<1433::AID-JOC203>3.0.CO;2-P.

Josey, S.A., Grist, J.P., Kieke, D., Yashayaev, I., Yu, L., 2015. [Global Oceans] Extraordinary Ocean Cooling and New Dense Water Formation in the North Atlantic, [in "State of the Climate in 2014"]. *Bulletin of the American Meteorological Society* 96, S67–S68.

Joughin, I., Smith, B.E., Shean, D.E. and Floricioiu, D. (2014) Brief communication: further summer speedup of Jakobshavn Isbræ. *The Cryosphere*, 8, 209–214. https://doi.org/10.5194/tc-8-209-2014.

Joyce, T.M. and Zhang, R. (2010) On the path of the Gulf stream and the Atlantic meridional overturning circulation. *Journal of Climate*, 23, 3146–3154. https://doi.org/10.1175/2010JCLI3310.1.

Kampa, M. and Castanas, E. (2008) Human health effects of air pollution. *Environmental Pollution*, Proceedings of the 4th International Workshop on Biomonitoring of Atmospheric Pollution (With Emphasis on Trace Elements), 151, 362–367. https://doi.org/10.1016/j.envpol.2007.06.012.

Kanzow, T., Cunningham, S.A., Rayner, D., Hirschi, J.J.-M., Johns, W.E., Baringer, M.O., Bryden, H.L., Beal, L.M., Meinen, C.S. and Marotzke, J. (2007) Observed flow compensation associated with the MOC at 26.5 N in the Atlantic. *Science*, 317, 938–941. https://doi.org/10.1126/science.1141293.

Knight, J.R., Allan, R.J., Folland, C.K., Vellinga, M. and Mann, M.E. (2005) A signature of persistent natural thermohaline circulation cycles in observed climate. *Geophysical Research Letters*, 32, L20708. https://doi.org/10.1029/2005GL024233.

Knight, J.R., Folland, C.K. and Scaife, A.A. (2006) Climate impacts of the Atlantic multidecadal oscillation. *Geophysical Research Letters*, 33, L17706. https://doi.org/10.1029/2006GL026242.

Korhonen, H., Carslaw, K.S., Forster, P.M., Mikkonen, S., Gordon, N.D. and Kokkola, H. (2010) Aerosol climate feedback due to decadal increases in Southern Hemisphere wind speeds: aerosol feedback due to wind speed. *Geophysical Research Letters*, 37, L02805. https://doi.org/10.1029/2009GL041320.

Krabill, W., Hanna, E., Huybrechts, P., Abdalati, W., Cappelen, J., Csatho, B., Frederick, E., Manizade, S., Martin, C., Sonntag, J., Swift, R., Thomas, R. and Yungel, J. (2004) Greenland ice sheet: increased coastal thinning. *Geophysical Research Letters*, 31, L24402. https://doi.org/10.1029/2004GL021533.

Kuipers Munneke, P., Ligtenberg, S.R.M., Noël, B.P.Y., Howat, I.M., Box, J.E., Mosley-Thompson, E., McConnell, J.R., Steffen, K., Harper, J.T., Das, S.B. and van den Broeke, M.R. (2015) Elevation change of the Greenland ice sheet due to surface mass balance and firn processes, 1960–2014. *The Cryosphere*, 9, 2009–2025. https://doi.org/10.5194/tc-9-2009-2015.

Kwok, R., Cunningham, G.F., Wensnahan, M., Rigor, I., Zwally, H.J. and Yi, D. (2009) Thinning and volume loss of the Arctic Ocean sea ice cover: 2003–2008. *Journal of Geophysical Research, Oceans*, 114, C07005. https://doi.org/10.1029/2009JC005312.

Landerer, F.W., Wiese, D.N., Bentel, K., Boening, C. and Watkins, M.M. (2015) North Atlantic meridional overturning circulation variations from GRACE ocean bottom pressure anomalies. *Geophysical Research Letters*, 42, 2015GL065730. https://doi.org/10.1002/2015GL065730.

Lazier, J., Hendry, R., Clarke, A., Yashayaev, I. and Rhines, P. (2002) Convection and restratification in the Labrador Sea, 1990 2000. *Deep Sea Res. Part Oceanogr. Res.*, 49, 1819–1835. https://doi.org/10.1016/S0967-0637(02)00064-X.

Lewis, R. and Schwartz, E. (2004) *Sea Salt Aerosol Production: Mechanisms, Methods, Measurements and Models—A Critical Review, Geophysical Monograph Series*. Washington, DC: American Geophysical Union. https://doi.org/10.1029/GM152.

Li, Q., Jacob, D.J., Bey, I., Palmer, P.I., Duncan, B.N., Field, B.D., Martin, R.V., Fiore, A.M., Yantosca, R.M., Parrish, D.D., Simmonds, P.G. and Oltmans, S.J. (2002) Transatlantic transport of pollution and its effects on surface ozone in Europe and North America. *Journal of Geophysical Research: Atmospheres*, 107, ACH 4-1. https://doi.org/10.1029/2001JD001422.

Lindsay, R.W. and Zhang, J. (2005) The thinning of Arctic Sea ice, 1988–2003: have we passed a tipping point? *Journal of Climate*, 18, 4879–4894. https://doi.org/10.1175/JCLI3587.1.

Lozier, M.S., Gary, S.F. and Bower, A.S. (2013) Simulated pathways of the overflow waters in the North Atlantic: subpolar to subtropical export. *Deep-Sea Research Part II: Topical Studies in Oceanography*, 85, 147–153. https://doi.org/10.1016/j.dsr2.2012.07.037.

Maidens, A., Arribas, A., Scaife, A.A., MacLachlan, C., Peterson, D. and Knight, J. (2013) The influence of surface Forcings on prediction of the North Atlantic oscillation regime of winter 2010/11. *Monthly Weather Review*, 141, 3801–3813. https://doi.org/10.1175/MWR-D-13-00033.1.

Malley, C.S., Henze, D.K., Kuylenstierna, J.C.I., Vallack, H.W., Davila, Y., Anenberg, S.C., Turner, M.C. and Ashmore, M.R. (2017) Updated global estimates of respiratory mortality in adults ≥30 Years of age attributable to long-term ozone exposure. *Environmental Health Perspectives*, 125, 087021. https://doi.org/10.1289/EHP1390.

Marshall, A.G. and Scaife, A.A. (2009) Impact of the QBO on surface winter climate. *Journal of Geophysical Research*, 114, D18110. https://doi.org/10.1029/2009JD011737.

Mauritzen, C., Melsom, A. and Sutton, R.T. (2012) Importance of density-compensated temperature change for deep North Atlantic Ocean heat uptake. *Nature Geoscience*, 5, 905–910. https://doi.org/10.1038/ngeo1639.

McCarthy, G., Frajka-Williams, E., Johns, W.E., Baringer, M.O., Meinen, C.S., Bryden, H.L., Rayner, D., Duchez, A., Roberts, C. and Cunningham, S.A. (2012) Observed interannual variability of the Atlantic meridional overturning circulation at 26.5°N. *Geophysical Research Letters*, 39, L19609. https://doi.org/10.1029/2012GL052933.

McCarthy, G.D., Haigh, I.D., Hirschi, J.J.-M., Grist, J.P. and Smeed, D.A. (2015a) Ocean impact on decadal Atlantic climate variability revealed by sea-level observations. *Nature*, 521, 508–510. https://doi.org/10.1038/nature14491.

McCarthy, G.D., Menary, M.B., Mecking, J.V., Moat, B.I., Johns, W.E., Andrews, M., Rayner, D. and Smeed, D.A. (2017) The importance of deep, basinwide measurements in optimised Atlantic meridional overturning circulation observing arrays. *Journal of Geophysical Research*, 122, 1808–1826. https://doi.org/10.1002/2016JC01220.

McCarthy, G.D., Smeed, D.A., Johns, W.E., Frajka-Williams, E., Moat, B.I., Rayner, D., Baringer, M.O., Meinen, C.S., Collins, J. and Bryden, H.L. (2015b) Measuring the Atlantic meridional overturning circulation at 26°N. *Progress in Oceanography*, 130, 91–111. https://doi.org/10.1016/j.pocean.2014.10.006.

McMillan, M., Leeson, A., Shepherd, A., Briggs, K., Armitage, T.W.K., Hogg, A., Kuipers Munneke, P., van den Broeke, M., Noël, B., van de Berg, W.J., Ligtenberg, S., Horwath, M., Groh, A., Muir, A. and Gilbert, L. (2016) A high-resolution record of Greenland mass balance: high-resolution Greenland mass balance. *Geophysical Research Letters*, 43, 7002–7010. https://doi.org/10.1002/2016GL069666.

Menary, M.B., Hodson, D.L.R., Robson, J.I., Sutton, R.T. and Wood, R.A. (2015) A mechanism of internal decadal Atlantic Ocean variability in a high-resolution coupled climate model. *Journal of Climate*, 28, 7764–7785. https://doi.org/10.1175/JCLI-D-15-0106.1.

Menary, M.B., Roberts, C.D., Palmer, M.D., Halloran, P.R., Jackson, L., Wood, R.A., Mueller, W.A., Matei, D. and Lee, S.-K. (2013) Mechanisms of

aerosol-forced AMOC variability in a state of the art climate model. *Journal of Geophysical Research, Oceans*, 118, 2087–2096.

Merchant, C.J., Embury, O., Roberts-Jones, J., Fiedler, E., Bulgin, C.E., Corlett, G.K., Good, S., McLaren, A., Rayner, N., Morak-Bozzo, S. and Donlon, C. (2014) Sea surface temperature datasets for climate applications from phase 1 of the European Space Agency climate change initiative (SST CCI). *Geoscience Data Journal*, 1, 179–191. https://doi.org/10.1002/gdj3.20.

Mickley, L.J., Jacob, D.J. and Rind, D. (2001) Uncertainty in preindustrial abundance of tropospheric ozone: implications for radiative forcing calculations. *Journal of Geophysical Research: Atmospheres*, 106, 3389–3399. https://doi.org/10.1029/2000JD900594.

Monks, P.S., Archibald, A.T., Colette, A., Cooper, O., Coyle, M., Derwent, R., Fowler, D., Granier, C., Law, K.S., Mills, G.E., Stevenson, D.S., Tarasova, O., Thouret, V., von Schneidemesser, E., Sommariva, R., Wild, O. and Williams, M.L. (2015) Tropospheric ozone and its precursors from the urban to the global scale from air quality to short-lived climate forcer. *Atmospheric Chemistry and Physics*, 15, 8889–8973. https://doi.org/10.5194/acp-15-8889-2015.

Neu, J.L., Flury, T., Manney, G.L., Santee, M.L., Livesey, N.J. and Worden, J. (2014) Tropospheric ozone variations governed by changes in stratospheric circulation. *Nature Geoscience*, 7, 340–344. https://doi.org/10.1038/ngeo2138.

Nghiem, S.V., Hall, D.K., Mote, T.L., Tedesco, M., Albert, M.R., Keegan, K., Shuman, C.A., DiGirolamo, N.E. and Neumann, G. (2012) The extreme melt across the Greenland ice sheet in 2012. *Geophysical Research Letters*, 39, L20502. https://doi.org/10.1029/2012GL053611.

Nisbet, E.G., Dlugokencky, E.J., Manning, M.R., Lowry, D., Fisher, R.E., France, J.L., Michel, S.E., Miller, J.B., White, J.W.C., Vaughn, B., Bousquet, P., Pyle, J.A., Warwick, N.J., Cain, M., Brownlow, R., Zazzeri, G., Lanoisellé, M., Manning, A.C., Gloor, E., Worthy, D.E.J., Brunke, E.-G., Labuschagne, C., Wolff, E.W. and Ganesan, A.L. (2016) Rising atmospheric methane: 2007–2014 growth and isotopic shift. *Global Biogeochemical Cycles*, 30, 2016GB005406. https://doi.org/10.1002/2016GB005406.

NOAA (2017). Arctic Oscillation (AO) Index, Edited, National Oceanic and Atmospheric Administration [WWW Document]. Available at: https://www.ncdc.noaa.gov/teleconnections/ao/ [Accessed 18th May 2017].

Noël, B., van de Berg, W.J., van Wessem, J.M., van Meijgaard, E., van As, D., Lenaerts, J.T.M., Lhermitte, S., Kuipers Munneke, P., Smeets, C.J.P.P., van Ulft, L.H., van de Wal, R.S.W. and van den Broeke, M.R. (2018) Modelling the climate and surface mass balance of polar ice sheets using RACMO2—part 1: Greenland (1958–2016). *The Cryosphere*, 12, 811–831. https://doi.org/10.5194/tc-12-811-2018.

NSIDC (2016a). March Ends a most Interesting Winter [WWW Document]. Arct. Sea Ice News Anal. Available at: http://nsidc.org/arcticseaicenews/2016/04/march-ends-a-most-interesting-winter/ [Accessed 18th May 2017].

NSIDC (2016b). Sluggish Ice Growth in the Arctic [WWW Document]. Arct. Sea Ice News Anal. Available at: http://nsidc.org/arcticseaicenews/2016/11/ [Accessed 18th May 2017].

Oetjen, H., Payne, V.H., Neu, J.L., Kulawik, S.S., Edwards, D.P., Eldering, A., Worden, H.M. and Worden, J.R. (2016) A joint data record of tropospheric ozone from Aura-TES and MetOp-IASI. *Atmospheric Chemistry and Physics*, 16, 10229–10239. https://doi.org/10.5194/acp-16-10229-2016.

Omrani, N.-E., Bader, J., Keenlyside, N.S. and Manzini, E. (2016) Troposphere–stratosphere response to large-scale North Atlantic Ocean variability in an atmosphere/ocean coupled model. *Climate Dynamics*, 46, 1397–1415. https://doi.org/10.1007/s00382-015-2654-6.

O'Reilly, C.H., Minobe, S., Kuwano-Yoshida, A. and Woollings, T. (2017) The Gulf stream influence on wintertime North Atlantic jet variability. *Quarterly Journal of the Royal Meteorological Society*, 143, 173–183. https://doi.org/10.1002/qj.2907.

Ortega, P., Hawkins, E. and Sutton, R. (2011) Processes governing the predictability of the Atlantic meridional overturning circulation in a coupled GCM. *Climate Dynamics*, 37, 1771–1782. https://doi.org/10.1007/s00382-011-1025-1.

Ortega, P., Lehner, F., Swingedouw, D., Masson-Delmotte, V., Raible, C.C., Casado, M. and Yiou, P. (2015) A model-tested North Atlantic oscillation reconstruction for the past millennium. *Nature*, 523, 71–74. https://doi.org/10.1038/nature14518.

Overland, J., Francis, J.A., Hall, R., Hanna, E., Kim, S.-J. and Vihma, T. (2015) The melting Arctic and Midlatitude weather patterns: are they connected?*. *Journal of Climate*, 28, 7917–7932. https://doi.org/10.1175/JCLI-D-14-00822.1.

Parrish, D.D., Lamarque, J.-F., Naik, V., Horowitz, L., Shindell, D.T., Staehelin, J., Derwent, R., Cooper, O.R., Tanimoto, H., Volz-Thomas, A., Gilge, S., Scheel, H.-E., Steinbacher, M. and Fröhlich, M. (2014) Long-term changes in lower tropospheric baseline ozone concentrations: comparing chemistry-climate models and observations at northern midlatitudes. *Journal of Geophysical Research: Atmospheres*, 119, 5719–5736. https://doi.org/10.1002/2013JD021435.

Pascoe, C.L., Gray, L.J. and Scaife, A.A. (2006) A GCM study of the influence of equatorial winds on the timing of sudden stratospheric warmings. *Geophysical Research Letters*, 33, L06825. https://doi.org/10.1029/2005GL024715.

Pausata, F.S.R., Pozzoli, L., Vignati, E. and Dentener, F.J. (2012) North Atlantic oscillation and tropospheric ozone variability in Europe: model analysis and measurements intercomparison. *Atmospheric Chemistry and Physics*, 12, 6357–6376. https://doi.org/10.5194/acp-12-6357-2012.

PCC. (2013) Climate change 2013: the physical science basis. In: Stocker, T.F., Qin, D., Plattner, G.K., Tignor, M., Allen, S.K., Boschung, J., Nauels, A., Xia, Y., Bex, V. and Midgley, P.M. (Eds.) *Contribution of Working Group I to the Fifth Assessment Report of the Intergovernmental Panel on Climate Change*. Cambridge, UK and New York, NY: Cambridge University Press, p. 1535. https://doi:10.1017/CBO9781107415324.

Peings, Y. and Magnusdottir, G. (2014) Forcing of the wintertime atmospheric circulation by the multidecadal fluctuations of the North Atlantic Ocean. *Environmental Research Letters*, 9, 034018. https://doi.org/10.1088/1748-9326/9/3/034018.

Perovich, D., Meier, W., Tschudi, M., Farrel, S., Hendricks, S., Gerland, S., Haas, C., Krumpen, T., Polashenski, C., Ricker, R., Webster, M. (2017). Sea Ice, in: Arctic Report Card 2017. http://www.arctic.noaa.gov/Report-Card.

Poulsen, C.A., Watts, P.D., Thomas, G.E., Sayer, A.M., Siddans, R., Grainger, R.G., Lawrence, B.N., Campmany, E., Dean, S.M. and Arnold, C. (2011) Cloud retrievals from satellite data using optimal estimation: evaluation and application to ATSR. *Atmospheric Measurement Techniques Discussions*, 4, 2389–2431. https://doi.org/10.5194/amtd-4-2389-2011.

Prather, M.J. and Holmes, C.D. (2017) Overexplaining or underexplaining methane's role in climate change. *Proceedings of the National Academy of Sciences of the United States of America*, 114, 5324–5326. https://doi.org/10.1073/pnas.1704884114.

Read, K.A., Mahajan, A.S., Carpenter, L.J., Evans, M.J., Faria, B.V.E., Heard, D.E., Hopkins, J.R., Lee, J.D., Moller, S.J., Lewis, A.C., Mendes, L., McQuaid, J.B., Oetjen, H., Saiz-Lopez, A., Pilling, M.J. and Plane, J.M.C. (2008) Extensive halogen-mediated ozone destruction over the tropical Atlantic Ocean. *Nature*, 453, 1232–1235. https://doi.org/10.1038/nature07035.

Rigby, M., Montzka, S.A., Prinn, R.G., White, J.W.C., Young, D., O'Doherty, S., Lunt, M.F., Ganesan, A.L., Manning, A.J., Simmonds, P.G., Salameh, P.K., Harth, C.M., Mhle, J., Weiss, R.F., Fraser, P.J., Steele, L.P., Krummel, P.B., McCulloch, A. and Park, S. (2017) Role of atmospheric oxidation in recent methane growth. *Proceedings of the National Academy of Sciences of the United States of America*, 114, 5373–5377. https://doi.org/10.1073/pnas.1616426114.

Rignot, E., Koppes, M. and Velicogna, I. (2010) Rapid submarine melting of the calving faces of West Greenland glaciers. *Nature Geoscience*, 3, 187–191. https://doi.org/10.1038/ngeo765.

Rignot, E., Velicogna, I., van den Broeke, M.R., Monaghan, A. and Lenaerts, J.T.M. (2011) Acceleration of the contribution of the Greenland and Antarctic ice sheets to sea level rise: acceleration of ice sheet loss. *Geophysical Research Letters*, 38, L05503. https://doi.org/10.1029/2011GL046583.

Roberts, C.D., Waters, J., Peterson, K.A., Palmer, M.D., McCarthy, G.D., Frajka-Williams, E., Haines, K., Lea, D.J., Martin, M.J., Storkey, D., Blockley, E.W. and Zuo, H. (2013) Atmosphere drives recent interannual variability of the Atlantic meridional overturning circulation at 26.5°N. *Geophysical Research Letters*, 40, 5164–5170. https://doi.org/10.1002/grl.50930.

Roberts, J.F., Champion, A.J., Dawkins, L.C., Hodges, K.I., Shaffrey, L.C., Stephenson, D.B., Stringer, M.A., Thornton, H.E. and Youngman, B.D. (2014) The XWS open access catalogue of extreme European windstorms from 1979 to 2012. *Natural Hazards and Earth System Sciences*, 14, 2487–2501. https://doi.org/10.5194/nhess-14-2487-2014.

Robson, J., Hodson, D., Hawkins, E. and Sutton, R. (2014) Atlantic overturning in decline? *Nature Geoscience*, 7, 2–3. https://doi.org/10.1038/ngeo2050.

Robson, J., Ortega, P. and Sutton, R. (2016) A reversal of climatic trends in the North Atlantic since 2005. *Nature Geoscience*, 9, 513–517. https://doi.org/10.1038/ngeo2727.

Robson, J., Sutton, R., Lohmann, K., Smith, D. and Palmer, M.D. (2012) Causes of the rapid warming of the North Atlantic Ocean in the mid-1990s. *Journal of Climate*, 25, 4116–4134. https://doi.org/10.1175/JCLI-D-11-00443.1.

Scaife, A.A., Comer, R., Dunstone, N., Fereday, D., Folland, C., Good, E., Gordon, M., Hermanson, L., Ineson, S., Karpechko, A., Knight, J., MacLachlan, C., Maidens, A., Peterson, K.A., Smith, D., Slingo, J. and Walker, B. (2017) Predictability of European winter 2015/2016. *Atmospheric Science Letters*, 18, 38–44. https://doi.org/10.1002/asl.721.

Scaife, A.A., Folland, C.K., Alexander, L.V., Moberg, A. and Knight, J.R. (2008) European climate extremes and the North Atlantic Oscillation. *Journal of Climate*, 21, 72–83. https://doi.org/10.1175/2007JCLI1631.1.

Scaife, A.A., Knight, J.R., Vallis, G.K. and Folland, C.K. (2005) A stratospheric influence on the winter NAO and North Atlantic surface climate. *Geophysical Research Letters*, 32, L18715. https://doi.org/10.1029/2005GL023226.

Schaefer, H., Fletcher, S.E.M., Veidt, C., Lassey, K.R., Brailsford, G.W., Bromley, T.M., Dlugokencky, E.J., Michel, S.E., Miller, J.B., Levin, I., Lowe, D.C., Martin, R.J., Vaughn, B.H. and White, J.W.C. (2016) A 21st century shift from fossil-fuel to biogenic methane emissions indicated by 13CH4. *Science*, 352, 80–84. https://doi.org/10.1126/science.aad2705.

Screen, J.A., Deser, C., Smith, D.M., Zhang, X., Blackport, R., Kushner, P.J., Oudar, T., McCusker, K.E. and Sun, L. (2018) Consistency and discrepancy in the atmospheric response to Arctic sea-ice loss across climate models. *Nature Geoscience*, 11, 155–163. https://doi.org/10.1038/s41561-018-0059-y.

Screen, J.A. and Simmonds, I. (2010) The central role of diminishing sea ice in recent Arctic temperature amplification. *Nature*, 464, 1334–1337. https://doi.org/10.1038/nature09051.

Seager, R., Kushnir, Y., Nakamura, J., Ting, M. and Naik, N. (2010) Northern hemisphere winter snow anomalies: ENSO, NAO and the winter of 2009/10. *Geophysical Research Letters*, 37, L14703. https://doi.org/10.1029/2010GL043830.

Semenov, V.A., Latif, M., Jungclaus, J.H. and Park, W. (2008) Is the observed NAO variability during the instrumental record unusual? *Geophysical Research Letters*, 35, L11701. https://doi.org/10.1029/2008GL033273.

Serreze, M.C. and Barry, R.G. (2005) *The Arctic Climate System*. Cambridge: Cambridge University Press. https://doi.org/10.1017/CBO9780511535888.

Shepherd, A., Ivins, E.R., Geruo, A., Barletta, V.R., Bentley, M.J., Bettadpur, S., Briggs, K.H., Bromwich, D.H., Forsberg, R., Galin, N., Horwath, M., Jacobs, S., Joughin, I., King, M.A., Lenaerts, J.T.M., Li, J., Ligtenberg, S.R.M., Luckman, A., Luthcke, S.B., McMillan, M., Meister, R., Milne, G., Mouginot, J., Muir, A., Nicolas, J.P., Paden, J., Payne, A.J., Pritchard, H., Rignot, E., Rott, H., Sorensen, L.S., Scambos, T.A., Scheuchl, B., Schrama, E.J.O., Smith, B., Sundal, A.V., van Angelen, J.H., van de Berg, W.J., van den Broeke, M.R., Vaughan, D.G., Velicogna, I., Wahr, J., Whitehouse, P.L., Wingham, D.J., Yi, D., Young, D. and Zwally, H.J. (2012) A reconciled estimate of ice-sheet mass balance. *Science*, 338, 1183–1189. https://doi.org/10.1126/science.1228102.

Shindell, D., Faluvegi, G., Lacis, A., Hansen, J., Ruedy, R. and Aguilar, E. (2006) Role of tropospheric ozone increases in 20th-century climate change. *Journal of Geophysical Research*, 111, D08302. https://doi.org/10.1029/2005JD006348.

Simmonds, P.G., Manning, A.J., Athanassiadou, M., Scaife, A.A., Derwent, R.G., O'Doherty, S., Harth, C.M., Weiss, R.F., Dutton, G.S., Hall, B.D., Sweeney, C. and Elkins, J.W. (2013) Interannual fluctuations in the seasonal cycle of nitrous oxide and chlorofluorocarbons due to the brewer-Dobson circulation: seasonal Amplitude of N_2O and CFCs. *Journal of Geophysical Research – Atmospheres*, 118(10), 694–10,706. https://doi.org/10.1002/jgrd.50832.

Smeed, D.A., McCarthy, G.D., Cunningham, S.A., Frajka-Williams, E., Rayner, D., Johns, W.E., Meinen, C.S., Baringer, M.O., Moat, B.I., Duchez, A. and Bryden, H.L. (2014) Observed decline of the Atlantic meridional overturning circulation 2004-2012. *Ocean Science*, 10, 29–38. https://doi.org/10.5194/os-10-29-2014.

Smith, D.M., Eade, R., Dunstone, N.J., Fereday, D., Murphy, J.M., Pohlmann, H. and Scaife, A.A. (2010) Skilful multi-year predictions of Atlantic hurricane frequency. *Nature Geoscience*, 3, 846–849. https://doi.org/10.1038/ngeo1004.

Stephens, G.L., Gabriel, P.M. and Partain, P.T. (2001) Parameterization of atmospheric radiative transfer. Part I: validity of simple models. *Journal of the Atmospheric Sciences*, 58, 3391–3409. https://doi.org/10.1175/1520-0469(2001)058<3391:POARTP>2.0.CO;2.

Stevenson, D.S., Young, P.J., Naik, V., Lamarque, J.-F., Shindell, D.T., Voulgarakis, A., Skeie, R.B., Dalsoren, S.B., Myhre, G., Berntsen, T.K., Folberth, G.A., Rumbold, S.T., Collins, W.J., MacKenzie, I.A., Doherty, R.M., Zeng, G., van Noije, T.P.C., Strunk, A., Bergmann, D., Cameron-Smith, P., Plummer, D.A., Strode, S.A., Horowitz, L., Lee, Y.H., Szopa, S., Sudo, K., Nagashima, T., Josse, B., Cionni, I., Righi, M., Eyring, V., Conley, A., Bowman, K.W., Wild, O. and Archibald, A. (2013) Tropospheric ozone changes, radiative forcing and attribution to emissions in the atmospheric chemistry and climate model Intercomparison project (ACCMIP). *Atmospheric Chemistry and Physics*, 13, 3063–3085. https://doi.org/10.5194/acp-13-3063-2013.

Strong, C. and Magnusdottir, G. (2011) Dependence of NAO variability on coupling with sea ice. *Climate Dynamics*, 36, 1681–1689. https://doi.org/10.1007/s00382-010-0752-z.

Sutton, R.T. and Dong, B. (2012) Atlantic Ocean influence on a shift in European climate in the 1990s. *Nature Geoscience*, 5, 788–792. https://doi.org/10.1038/ngeo1595.

Sutton, R.T. and Hodson, D.L.R. (2005) Atlantic Ocean forcing of north American and European summer climate. *Science*, 309, 115–118. https://doi.org/10.1126/science.1109496.

Sutton, R.T., McCarthy, G.D., Robson, J., Sinha, B., Archibald, A. and Gray, L.J. (2017) Atlantic multi-decadal variability and the UK ACSIS programme. *Bulletin of the American Meteorological Society*, 99, 415–425. https://doi.org/10.1175/BAMS-D-16-0266.1.

Swingedouw, D., Rodehacke, C.B., Behrens, E., Menary, M., Olsen, S.M., Gao, Y., Mikolajewicz, U., Mignot, J. and Biastoch, A. (2013) Decadal fingerprints of freshwater discharge around Greenland in a multi-model ensemble. *Climate Dynamics*, 41, 695–720. https://doi.org/10.1007/s00382-012-1479-9.

Taylor, P.C., Cai, M., Hu, A., Meehl, J., Washington, W. and Zhang, G.J. (2013) A decomposition of feedback contributions to polar warming amplification. *Journal of Climate*, 26, 7023–7043. https://doi.org/10.1175/JCLI-D-12-00696.1.

Tedesco, M., Mote, T., Fettweis, X., Hanna, E., Jeyaratnam, J., Booth, J.F., Datta, R. and Briggs, K. (2016) Arctic cut-off high drives the poleward shift of a new Greenland melting record. *Nature Communications*, 7, 11723. https://doi.org/10.1038/ncomms11723.

Thomas, R., Frederick, E., Krabill, W., Manizade, S. and Martin, C. (2006) Progressive increase in ice loss from Greenland: increase in ice loss from Greenland. *Geophysical Research Letters*, 33, L10503. https://doi.org/10.1029/2006GL026075.

Thornalley, D.J.R., Oppo, D.W., Ortega, P., Robson, J.I., Brierley, C.M., Davis, R., Hall, I.R., Moffa-Sanchez, P., Rose, N.L., Spooner, P.T., Yashayaev, I. and Keigwin, L.D. (2018) Anomalously weak Labrador Sea convection and Atlantic overturning during the past 150 years. *Nature*, 556, 227–230. https://doi.org/10.1038/s41586-018-0007-4.

Tian, B., Manning, E., Fetzer, E., Olsen, E., Wong, S., Susskind, J., Iredell, L. (2017). AIRS/AMSU/HSB Version 6 Level 3 Product User Guide. Version 1.3.2.

Tilling, R.L., Ridout, A. and Shepherd, A. (2016) Near-real-time Arctic sea ice thickness and volume from CryoSat-2. *The Cryosphere*, 10, 2003–2012. https://doi.org/10.5194/tc-10-2003-2016.

Tilling, R.L., Ridout, A., Shepherd, A. and Wingham, D.J. (2015) Increased Arctic sea ice volume after anomalously low melting in 2013. *Nature Geoscience*, 8, 643–646. https://doi.org/10.1038/ngeo2489.

Turner, A.J., Frankenberg, C., Wennberg, P.O. and Jacob, D.J. (2017) Ambiguity in the causes for decadal trends in atmospheric methane and hydroxyl. *Proceedings of the National Academy of Sciences of the United States of America*, 114, 5367–5372. https://doi.org/10.1073/pnas.1616020114.

Twomey, S. (1974) Pollution and the planetary albedo. *Atmospheric Environment*, 1967(8), 1251–1256. https://doi.org/10.1016/0004-6981(74)90004-3.

van den Broeke, M., Bamber, J., Ettema, J., Rignot, E., Schrama, E., van de Berg, W.J., van Meijgaard, E., Velicogna, I. and Wouters, B. (2009) Partitioning recent Greenland mass loss. *Science*, 326, 984–986. https://doi.org/10.1126/science.1178176.

van den Broeke, M., Box, J., Fettweis, X., Hanna, E., Noël, B., Tedesco, M., van As, D., van de Berg, W.J. and van Kampenhout, L. (2017) Greenland ice sheet surface mass loss: recent developments in observation and modeling. *Current Climate Change Reports*, 3, 345–356. https://doi.org/10.1007/s40641-017-0084-8.

Vaughan, D.G., Comiso, J.C., Allison, I., Carrasco, J., Kaser, G., Kwok, R., Mote, P., Murray, T., Paul, F., Ren, J. and Rignot, E. (2013) Observations: cryosphere. In: *Climate Change 2013: Physical Science Basis. Contribution of Working Group I to the Fifth Assessment Report of the Intergovernmental Panel on Climate Change*. Cambridge, UK: Cambridge University Press.

Wang, L., Ting, M. and Kushner, P.J. (2017) A robust empirical seasonal prediction of winter NAO and surface climate. *Scientific Reports*, 7, 279. https://doi.org/10.1038/s41598-017-00353-y.

Watson, P.A.G., Weisheimer, A., Knight, J.R. and Palmer, T.N. (2016) The role of the tropical West Pacific in the extreme northern hemisphere winter of 2013/2014. *Journal of Geophysical Research – Atmospheres*, 121, 1698–1714. https://doi.org/10.1002/2015JD024048.

Welti, A., Müller, K., Fleming, Z.L. and Stratmann, F. (2017) Concentration and variability of ice nuclei in the subtropical, maritime boundary layer. *Atmospheric Chemistry and Physics*, 18, 5307–5320. https://doi.org/10.5194/acp-2017-783.

Wigley, T.M.L., Santer, B.D. and Lanzante, J.R. (2006) Appendix A: statistical issues regarding trends. In: Karl, T.R. , Hassol, S.J. , Miller, C.D. and Murray, W.L. (Eds.) *Temperature Trends in the Lower Atmosphere: Steps for Understanding and Reconciling Differences*. Washington DC: A Report by the U.S. Climate Change Science Program and the Subcommittee on Global Change Research.

Wild, S., Befort, D.J. and Leckebusch, G.C. (2015) Was the extreme storm season in winter 2013/14 over the North Atlantic and the United Kingdom triggered by changes in the West Pacific warm pool? *Bulletin of the American Meteorological Society*, 96, S29–S34. https://doi.org/10.1175/BAMS-D-15-00118.1.

Williams, R.G., Roussenov, V., Smith, D. and Lozier, M.S. (2014) Decadal evolution of ocean thermal anomalies in the North Atlantic: the effects of Ekman, overturning, and horizontal transport. *Journal of Climate*, 27, 698–719. https://doi.org/10.1175/JCLI-D-12-00234.1.

Wingham, D.J., Francis, C.R., Baker, S., Bouzinac, C., Brockley, D., Cullen, R., de Chateau-Thierry, P., Laxon, S.W., Mallow, U., Mavrocordatos, C., Phalippou, L., Ratier, G., Rey, L., Rostan, F., Viau, P. and Wallis, D.W. (2006) CryoSat: a mission to determine the fluctuations in Earth's land and marine ice fields. *Advances in Space Research*, Natural Hazards and Oceanographic Processes from Satellite Data, 37, 841–871. https://doi.org/10.1016/j.asr.2005.07.027.

Winton, M. (2006) Amplified Arctic climate change: What does surface albedo feedback have to do with it? *Geophysical Research Letters*, 33, L03701. https://doi.org/10.1029/2005GL025244.

Woollings, T., Czuchnicki, C. and Franzke, C. (2014) Twentieth century North Atlantic jet variability: jet variability. *Quarterly Journal of the Royal Meteorological Society*, 140, 783–791. https://doi.org/10.1002/qj.2197.

Woollings, T., Franzke, C., Hodson, D.L.R., Dong, B., Barnes, E.A., Raible, C.C. and Pinto, J.G. (2015) Contrasting interannual and multidecadal NAO variability. *Climate Dynamics*, 45, 539–556.

Woollings, T., Gregory, J.M., Pinto, J.G., Reyers, M. and Brayshaw, D.J. (2012) Response of the North Atlantic storm track to climate change shaped by ocean-atmosphere coupling. *Nature Geoscience*, 5, 313–317.

Worden, H.M., Deeter, M.N., Frankenberg, C., George, M., Nichitiu, F., Worden, J., Aben, I., Bowman, K.W., Clerbaux, C., Coheur, P.F., de Laat, A.T.J., Detweiler, R., Drummond, J.R., Edwards, D.P., Gille, J.C., Hurtmans, D., Luo, M., Martínez-Alonso, S., Massie, S., Pfister, G. and Warner, J.X. (2013) Decadal record of satellite carbon monoxide observations. *Atmospheric Chemistry and Physics*, 13, 837–850. https://doi.org/10.5194/acp-13-837-2013.

Xiong, X., Barnet, C., Maddy, E., Sweeney, C., Liu, X., Zhou, L. and Goldberg, M. (2008) Characterization and validation of methane products from the atmospheric Infrared sounder (AIRS). *Journal of Geophysical Research*, 113, G00A01. https://doi.org/10.1029/2007JG000500.

Yashayaev, I. and Loder, J.W. (2016) Recurrent replenishment of Labrador Sea water and associated decadal-scale variability: 2015 convection in Labrador Sea. *Journal of Geophysical Research, Oceans*, 121, 8095–8114. https://doi.org/10.1002/2016JC012046.

Yashayaev, I., van Aken, H.M., Holliday, N.P. and Bersch, M. (2007) Transformation of the Labrador Sea water in the subpolar North Atlantic. *Geophysical Research Letters*, 34, L22605. https://doi.org/10.1029/2007GL031812.

Young, P.J., Archibald, A.T., Bowman, K.W., Lamarque, J.-F., Naik, V., Stevenson, D.S., Tilmes, S., Voulgarakis, A., Wild, O., Bergmann, D., Cameron-Smith, P., Cionni, I., Collins, W.J., Dalsøren, S.B., Doherty, R.M., Eyring, V., Faluvegi, G., Horowitz, L.W., Josse, B., Lee, Y.H., MacKenzie, I.A., Nagashima, T., Plummer, D.A., Righi, M., Rumbold, S.T., Skeie, R.B., Shindell, D.T., Strode, S.A., Sudo, K., Szopa, S. and Zeng, G. (2013) Pre-industrial to end 21st century projections of tropospheric ozone from the atmospheric chemistry and climate model Intercomparison project (ACCMIP). *Atmospheric Chemistry and Physics*, 13, 2063–2090. https://doi.org/10.5194/acp-13-2063-2013.

Yuan, T., Oreopoulos, L., Zelinka, M., Yu, H., Norris, J.R., Chin, M., Platnick, S. and Meyer, K. (2016) Positive low cloud and dust feedbacks amplify tropical North Atlantic Multidecadal Oscillation. *Geophysical Research Letters*, 43, 1349–1356. https://doi.org/10.1002/2016GL067679.

Yurganov, L.N., McMillan, W.W., Dzhola, A.V., Grechko, E.I., Jones, N.B. and van der Werf, G.R. (2008) Global AIRS and MOPITT CO measurements: validation, comparison, and links to biomass burning variations and carbon cycle. *Journal of Geophysical Research*, 113, D09301. https://doi.org/10.1029/2007JD009229.

Zhang, J.L. and Rothrock, D.A. (2003) Modeling global sea ice with a thickness and enthalpy distribution model in generalized curvilinear coordinates. *Monthly Weather Review*, 131, 845–861. https://doi.org/10.1175/1520-0493(2003)131<0845:MGSIWA>2.0.CO;2.

Zhang, R. and Delworth, T.L. (2006) Impact of Atlantic multidecadal oscillations on India/Sahel rainfall and Atlantic hurricanes. *Geophysical Research Letters*, 33, D09301. https://doi.org/10.1029/2006GL026267.

Ziemke, J.R., Chandra, S., Duncan, B.N., Froidevaux, L., Bhartia, P.K., Levelt, P.F. and Waters, J.W. (2006) Tropospheric ozone determined from Aura OMI and MLS: evaluation of measurements and comparison with the global modeling Initiative's chemical transport model. *Journal of Geophysical Research*, 111, D19303. https://doi.org/10.1029/2006JD007089.

SUPPORTING INFORMATION

Additional supporting information may be found online in the Supporting Information section at the end of the article.

How to cite this article: Robson J, Sutton RT, Archibald A, *et al.* Recent multivariate changes in the North Atlantic climate system, with a focus on 2005–2016. *Int J Climatol*. 2018;1–27. https://doi.org/10.1002/joc.5815